Regulation of the Potassium channels Kv1.3, Kv1.5 and Kir2.1 by Human Parvovirus B19 Capsid Protein VP1

Inaugural-Dissertation

Zur Erlangung des Doktorgrades

der Medizin

Der medizinischen Fakultät

der Eberhard Karls Universität

zu Tübingen

vorgelegt von

Sedig Ahmed, Musaab

2016

To the soul of my grandfather.

To my family and my friends for always being there throughout my hardship, pains and happiness.

Table of contents

List of tables

List of Figures

VIII

List of abbreviations

B19V	parvovirus B19
cRNA	circular RNA
DEPC	Diethylpyrocarbonate
E_{res}	resting membrane potential
HEPES	4-(2-hydroxyethyl)-1-piperazineethanesulfonic acid
I_K	Kir current
ITP	idiopathic thrombocytopenic purpura
I/V	current/voltage
Kv	voltage gated Potassium channel
mV	millivolt
nm	nanometer
ND96	Physiological Ringer solution
nt	nucleotide
NS1	major nonstructural protein
PCR	polymerase chain reaction
PLA2	phospholipase A2
pS	picosiemens
s	second
TEVC	two electrode voltage clamp

1. Introduction

1.1 Human Parvovirus B19

Parvovirus B19 (B19V) was discovered by the Australian Virologist, Yvonne Cossart while screening sera from blood bank for hepatitis B virus in 1974 (1). The name B19 was originated from the coding of a serum sample occupying position 19 in panel B that gave inconsistent results when it was tested for hepatitis B (1). B19V is a small nonenveloped virus of about 22 to 24 nm in diameter. It is classified as a member of the genus Erythrovirus within the family of Parvoviridae (2).

1.1.1 Genomic structure and organization of B19V

The single stranded genome includes 5,596 nucleotides (nt), composed of an internal coding sequence of 4,830 nt flanked by the terminal repeat sequences of 383 nt each (3). The B19V genome has two large open reading frames, with the two capsid proteins VP1 and VP2 encoded by genes on the right side and the single nonstructural protein (NS1) encoded by genes on the left side of the genome. Transcription is capable for producing at least nine overlapping mRNA transcripts, all of them arise from the single P6 promoter at the extreme left side of the genome (3-5). The most important viral proteins include the major nonstructural protein NS1 and the two structural proteins VP1 and VP2 (5, 6).

1.1.1.1 Nonstructural protein and capsid proteins

The major nonstructural protein, NS1 (nt 435 to 2448) has a molecular mass of 77 kDa (5-8). The NS1 protein may function to have site specific DNA binding, DNA nicking, ATPase, transcriptional, and helicase activities (9-13), transactivator of cellular and viral promoters (14), stimulator of apoptosis (15-17), and modulates inflammatory signaling by activation of the STAT3/PIAS3 pathway (18).

The B19V genome further encodes the structural capsid proteins VP1 and VP2 (6), which are decisive for the viral life cycle (19, 20). The VP2 protein is encoded by sequences from nt 3125 to 4786 and has a molecular mass of 58 kDa. VP1 is the minor capsid protein encoded by the sequence from nt 2444 to 4786 and is identical to VP2 with the addition of 227 amino acids (termed the VP1 unique region) at the amino terminus (7, 8). The VP1 has a molecular mass of 84 kDa and makes up 4% of the total capsid protein (7).

The VP1 protein contains a sequence similar to secreted phospholipase A2 (sPLA2) (21-23), which probably generates eicosanoids (23, 24). The vPLA2 enzyme activity is disrupted by replacement of a histidine at position 153 with alanine ([H153A]VP1) (23, 24).
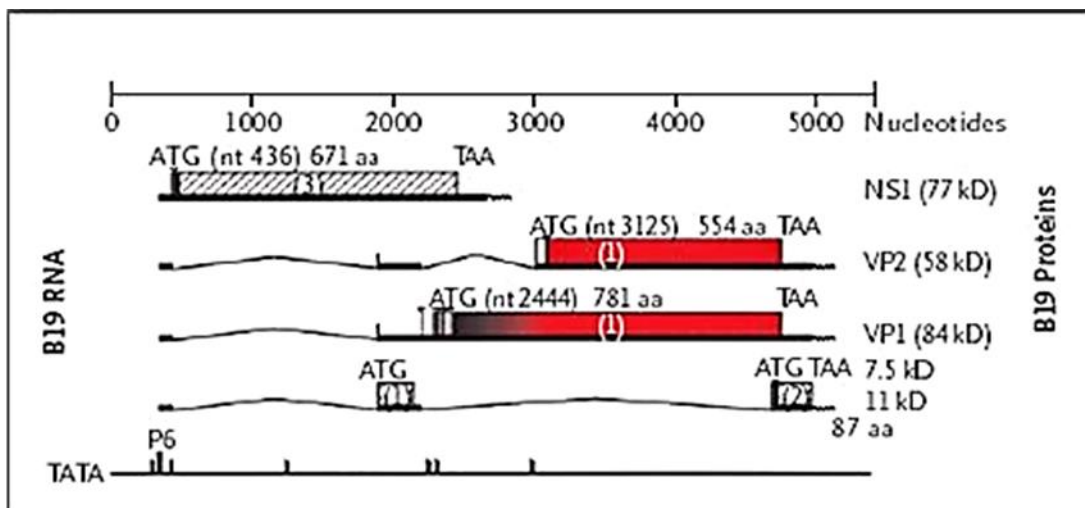
Figure 1: Transcription map of the major genes and resulting transcripts of B19. The nonstructural protein NS1 arises from the single unspliced transcript on the left-hand side of the genome (hatched areas). The capsid proteins VP1 and VP2 are encoded by genes with overlapping reading frames from the right-hand side of the genome, aa denotes amino acids, nt nucleotides, (1), (2), and (3) reading frames, and P6, the single viral promoter (25).

1.1.2 Pathophysiology

The life cycle of B19V is similar to other nonenveloped DNA viruses in binding of the virus to the receptors of the host cell, internalization, translocation of the genome to the host nucleus, DNA replication, RNA transcription, assembly of

capsids and packaging of the genome, and finally lysis of the cell with release of the mature virions (2).
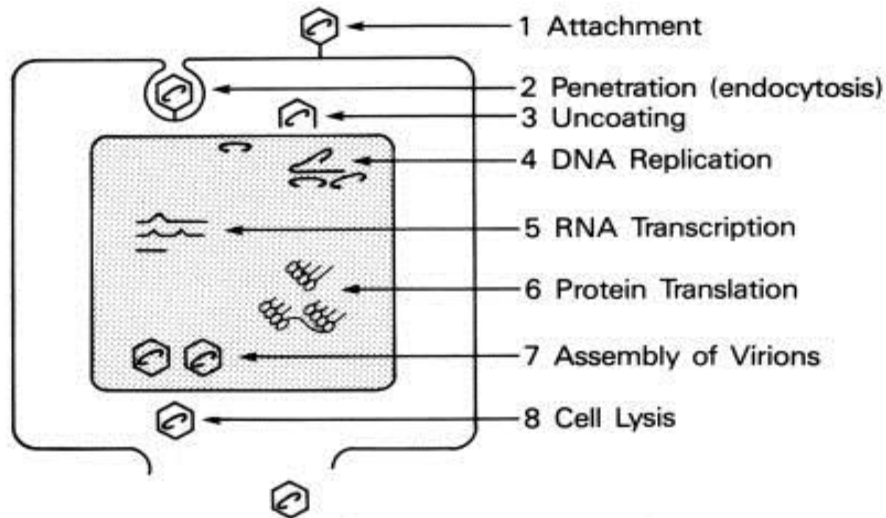
Figure 2: Schematic life cycle of Parvovirus B19 (2)

B19V replicates in erythroid progenitor cells (26) and has been shown to cause agglutination of human red cells (27) and to bind to blood group P antigen in erythroid progenitor cells, as measured by hemagglutination (26). In tissue culture anti-P monoclonal antibody has blocked infection of erythroid progenitors with B19V. Erythrocytes lacking P antigen are not agglutinated with B19 thus demonstrating that P antigen is the B19V receptor (26). P antigen is present also on megakaryocytes, endothelial cells, placenta and fetal liver. The tissue distribution of P antigen is consistent with the clinical syndromes caused by parvovirus B19. People lacking P antigen are resistant to B19 infection (28).

B19V may enter cells by binding to blood group P antigen (29), α5β1 integrin and Ku80 autoantigen (30, 31). B19V thus preferably invades erythroid progenitor cells but may enter fetal myocytes, follicular dendritic cells and endothelial cells (29-32). In fatal inflammatory cardiomyopathy the virus is particularly abundant in endothelial cells (33, 34).

1.1.3 Prevalence and Incidence

B19V is a worldwide infectious pathogen in humans. The estimated prevalence of IgG antibodies directed against B19V ranges from 2 to 15% in children at age of 1 to 5 years old, 15 to 60% in children aged 6 to 19 years old, 30 to 60% in adults, and more than 85% in the geriatric population (35-38). Women of the childbearing age have an annual seroconversion rate of 1.5% (39).

1.1.4 Transmission

Transmission of B19V infection can occur through the respiratory route, blood derived products administered parenterally, and from mother to fetus. The virus is generally spread in the community by a respiratory route as B19V specific DNA has been detected in the respiratory secretions at the time of viremia. The case to case interval is 6 to 11 days irrespective of the type of B19V related disease (2). Transmission from the mother to the fetus occurs in one third of cases involving serologically confirmed primary maternal infections (40). Nosocomial transmission has been shown infrequently (41). The transmission can also occur among staff in laboratories handling native virus (42).

1.1.5 Diseases associated with B19V

B19V diseases primarily involves infection in the healthy host manifested as fifth disease (erythema infectiosum), arthralgia, hydrops, myocarditis, neurologic disease, hepatitis as well as hematologic symptoms in predisposed individuals (2).

1.1.5 .1 Asymptomatic infection

The presence of subclinical B19V infection is a common finding in both children and adults. In 1989, it has been shown that quarter of infected persons had no recollection of specific symptoms (43) and In 1991, it has been shown that fewer than 50% of IgM-positive women show signs of rash or arthralgia (44). Asymptomatic seroconversion following recent transfusion in patients with

hemolytic anemia suggests that symptoms can be hidden by transfusion of erythrocytes with a longer life span than the defective erythrocytes of the host (45).

1.1.5.2 Fifth disease

Fifth disease is also known as Erythema infectiosum or slapped cheek disease. It is the commonest manifestation of B19V infection in children (46). The association with B19V has been identified Following an outbreak of fifth disease by the discovery of specific IgM in specimens from the involved patients (2). The disease starts with prodromal symptoms which often unnoticed including fever, coryza, headache and nausea. It is characterized by a facial erythema of medium intensity appearing in the cheeks with relative circumoral pallor (slapped cheek appearance) beginning 18 days after infection. The second stage is composed of a rash appearing in the limbs and trunk occurs 1 to 4 days later. The rash is reticular and composed of pink maculae that usually undergo a central fading, which causes the rash to develop a festooned appearance. The rash can be transient or recurrent, and the difference in intensity can be linked to environmental factors such as heat and exposure to sunlight (47). Other symptoms include scaly dermatitis, itching, vesicles (43, 48).

1.1.5.3 Arthropathy

The association between arthropathy and B19V infection has been identified in 1985 (49, 50). The incidence of arthralgia is approximately 10% or less in children with fifth disease, while 19% of children with recent arthritis have evidence of recent B19 infection (51).
Arthralgia and arthritis are the most prevalent manifestations of primary B19V infection in adults affecting 30% of males and 60% of females, while the dermal affection is less frequent and not characteristic in the adult population (43, 46, 52). The arthropathy is likely to be immunologically mediated since the onset exists with the appearance of circulating antibodies. Joint symptoms present as an acute

moderately severe peripheral polyarthritis involving the metacarpophalangeal joints (75%), wrists (55%), knees (65%), and ankles (40%) without articular erosions (53). About 50% of patients with chronic B19V arthropathy meet the criteria of the American Rheumatoid Association for a diagnosis of rheumatoid arthritis (54, 55).

1.1.5.4 Hydrops fetalis

It has been shown that B19V cause nonimmune hydrops fetalis (56). Fetal B19V infection may also cause fetal or congenital anemia, abortion, or stillbirth or result in an asymptomatic self limiting episode (2). It has been reported that B19V cause congenital malformations (57, 58). The pathogenesis of fetal damage is similar to that of patients with aplastic crisis in which the erythrocytes have a reduced life span. Erythroblasts in the fetal liver exhibit signs of B19V infection (59, 60). Fetal infection is persistent and characterized by severe anemia, high output cardiac failure, and death (61). Impaired circulation caused by fetal myocarditis may contribute to the accumulation of fluids (62).

The incidence rate of B19V infection during pregnancy is about 1 to 5% (63-65). The risk of developing hydrops following B19V infection is ranging from 0 to 24% (66-72), however, in pregnant women with a confirmed primary infection, the risk of an abnormal outcome is about 5 to 10% (40, 67, 71). The possblity of an adverse fetal outcome after infection is greatest between 11 and 23 weeks of gestation, which correlates with the hepatic period of hematopoietic activity (73, 74). Cordocentesis can give precise assessment of fetal anemia, which can be then corrected by intravenous transfusion of erythrocytes (75).

1.1.5.5 Myocarditis

B19V infection of cardiac endothelial cells may result in isolated left ventricular diastolic dysfunction (76) and is an important pathogenic agent in the etiology of inflammatory cardiomyopathy (iCMP) (77). B19V infection may occur during pregnancy leading to maternal and fetal myocarditis, congenital malformations,

stillbirth and abortion (78-81). The consequences of antenatal infections are particularly severe as B19V preferably enters proliferating cells (82). B19V thus preferably invades erythroid progenitor cells but may enter fetal myocytes, follicular dendritic cells and endothelial cells (29-32). In fatal inflammatory cardiomyopathy the virus was particularly abundant in endothelial cells (33, 34). B19 infection has been shown to cause general disease in pediatric cardiac transplant recipients (83, 84) as well as possible myocarditis (85, 86).

1.1.5.6 Neurologic disease

Association of neurologic symptoms with erythema infectiosum has been identified (87, 88). B19V DNA have been detected in cerebrospinal fluid in fatal encephalopathy (89) and aseptic meningitis (90). B19V antibodies were detected in complex regional pain syndrome (91). Neuralgic amyotrophy has been reported following B19V infection (92).

1.1.5.7 Hepatitis

B19V was first identified in a sample sent for hepatitis testing (2). B19V might cause hepatitis (93), transient disturbance of consciousness, hepatic dysfunction (94) , fulminant liver failure before or immediately after liver transplantation in children (95), acute hepatitis or hepatic disorder after B19 infection in adults (96).

1.1.5.8 Transient aplastic crisis

Transient aplastic crisis was the first disease to be associated with B19V. It is characterized by a short self limited episode of pure red cell aplasia which had been shown in patients with hemolytic anemia, however, any person suffering from decreased erythrocyte production or increased destruction or loss of erythrocytes might be in risk of developing aplastic crisis following B19V infection (2).

Moreover, conditions associated with decreased erythrocyte production predispose for the development of B19V induced aplastic crisis including iron deficiency(2), congenital dyserythropoietic anemia (97), and α- and β-thalassemias (98-101). B19V may also cause transient aplastic crisis in patients with increased erythrocyte destruction or loss diseases including hereditary spherocytosis (98, 101, 102), hereditary stomatocytosis (103), pyruvate kinase deficiency (104), pyrimidine-5′-nucleotidase deficiency (105), sickle cell disease (45, 98, 106), chronic autoimmune hemolytic anemia (100) and paroxysmal nocturnal hemoglobinuria (107).

1.1.5.9 Congenital anemia

It was reported that three infants with hydrops have congenital anemia due to transplacental B19 infection (108). B19V DNA has been detected in 3 of 11 Bone marrow smears, and giant pronormoblasts showed low sensitivity (33%) and poor specificity (75%) in children diagnosed with Diamond-Blackfan anemia which is a congenital anemia disorder (109). In another report, an infant developed congenital anemia due to a possible B19V infection (110).

1.1.5.10 Thrombocytopenia and Neutropenia

B19V infection may cause subclinical or overt thrombocytopenia in patients (46, 111-113). Recent B19V infection has been shown in 6 of 47 pediatric idiopathic thrombocytopenic purpura patients (ITP) (13%) and it has suggested that children with ITP and associated B19V infection are characterized by acute onset of thrombocytopenia. Among the B19V positive children, the duration of the illness was short in three children treated with immunoglobulin but chronic in the remaining three patients given high dose of steroids (114).

Examination of the bone marrow has showed that Parvovirus B19V infection might be a common cause of immune mediated neutropenia in childhood (115).

1.1.5.11 Transient erythroblastopenia of childhood

Transient erythroblastopenia of childhood (TEC) is a disorder characterized by anemia, reticulocytopenia, and decreased red blood cell precursors in the bone marrow aspiration affecting young children, age 3 to 4 years. TEC is a common cause of red cell aplasia in immunocompetent children. Due to its hematopoietic effect, B19V might be involved in this disorder (116-118).

1.1.6 Diagnosis of B19V

1.1.6.1 Diagnostic Cytopathology

The presence of giant pronormoblasts in either peripheral blood or bone marrow is suggestive of B19V infection, however, their presence or absence should not be considered as the only criteria for diagnosis of B19V infection (2).

1.1.6.2 Detection of B19 Virus

B19V can be detected by isolation of viral DNA using direct hybridization or PCR methods. Direct hybridization as a slot blot or dot blot format, generally employs an almost full length viral DNA probe labeled with ^{32}P, digoxigenin or biotin to bind to DNA in clinical specimens (119, 120). Direct hybridization is very sensitive to detect B19V levels in acute transient aplastic crisis (2).

PCR has increased the sensitivity of DNA detection (121-123). DNA can be detected for extended periods of time in serum (124-126), synovial membranes (127) and bone marrow (128). Detection of low levels of B19V DNA alone cannot be used for diagnosing acute B19V infection (2).

1.1.6.3 Detection of Antibodies

B19V IgM has been detected in over 85% of clinical cases of fifth disease and aplastic crisis With the IgM ELISA method. B19V IgG antibodies prevalence is

increased according to age. About 2% of children less than 5 years of age and 49% of adults greater than 20 years of age had B19V IgG antibodies. The B19V antibody ELISAs are specific and sensitive tests to detect B19 infections (35).

1.1.7 Treatment

In most cases, patients with fifth disease do not need any treatment while some patients with B19V arthralgia might need symptomatic treatment (anti-inflammatory drugs). The prognosis of transient aplastic crisis caused by B19V can be good by erythrocyte transfusion which improve the hemoglobin concentration (129). B19V infection in pregnant seronegative women must be monitored by weekly ultrasound examinations and cordocentesis. The mortality of hydrops fetalis can be lowered by intrauterine transfusions (75). The most Effective treatment for persistent B19V infection (pure red cell aplasia) is infusion of immunoglobulin (0.4 g/kg of body weight/day for 5 days or 1g/kg/day for 2 to 3 days). This treatment is very often curative leading to a marked rise in reticulocyte count and rise in hemoglobin concentration (130-133).

1.2 Potassium channels

Membrane proteins represent about 30% of the total proteome of an organism and the half of this number is carrier proteins and ion channels. Potassium ion channels are considered to be the most diverse and the predominant class of membrane proteins(134). The potassium channels are classified depending on the primary structure and the function into: voltage gated (Kv) channels, inwardly rectifying channels (Kir), Ca^{2+}-activated channels (KCa) and two-pore domain (K2P). Kv channels are the most diverse group of the potassium channels (135).

1.2.1 Voltage Gated Potassium Channels Kv1.3 and Kv1.5

Voltage gated K^+ channels (Kv), a superfamily that include 12 subfamilies (Kv1-Kv12), contribute to the maintenance of resting membrane potential and the control of action potentials (136).The voltage gated K^+ channels Kv1.3 and Kv1.5 are members of the Shaker (Kv1) family of K^+ channels and are involved in tissue differentiation and cell growth (137).

1.2.1.1 Structure of Kv Channels

All Kv channels share high level of similarity. Each Kv channel gene encodes one α-subunit (Kvα). Each four α-subunits form a functional channel. Kv channels are usually homotetrameric in structure (with all Kvα being identical) (138, 139), however, some channels can be heterotetrameric (with two or more non-identical Kvα subunits) (140).

The transmembrane domain of the Kv channel α-subunit is composed of six helices: S1-S6 These helices form two structurally and functionally different parts of the tetrameric channel: pore domain which is a potassium ion conducting domain formed by helices S5-S6 located in the channel center and voltage sensing domain, VSD which is sensible to changes in the membrane potential formed by helices S1-S4 located on the channel periphery (140).

The pore part has a channel gate and a selective filter that does not allow ions other than K^+ to pass through the channel. The channel gate is created by crossing C-termini of the S6 helices that block passage of ions when the channel is closed (141-143). The selective filter is formed by a conserved fragment (P-region) and a S5-S6 loop (140).

The pore domain and voltage-sensing domain (VSD) are covalently bound by the S4-S5 linker which is an amphiphylic helix connected to the C-terminus of S6 helix (S6T) and the next subunit (140, 144-148). The highly conserved region of the S6T helix plays an important role in the opening and closing of the channel. It is a flexible region which allows the channel to open (140).

Kv channels have two gates: the upper gate formed by the P-loop of the selectivity filter on the extracellular side and the lower gate formed by crossing the S6 helices on the intracellular side. In the Kv channels, lower gates are the main activation gates which are controlled by external stimuli, such as the membrane potential (140). Kv channels also have a cytoplasmic part which is formed by N- and C-termini beside the transmembrane part (149).
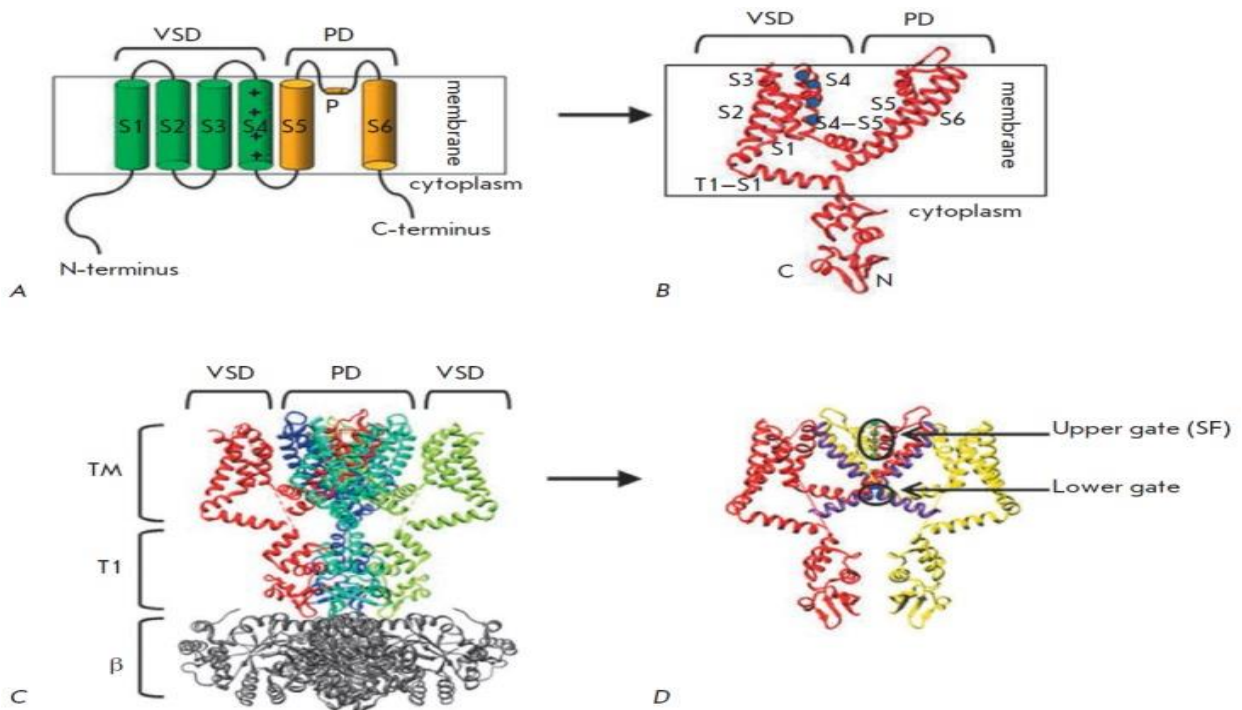
Figure 3: Structure of Kv channels. A. Scheme of a single α-subunit of the Kv channel. Transmembrane segments S1–S6 and pore-forming P-loop are marked. Charged Arg of the membrane voltage sensor S4 are marked with "+" signs. PD–pore domain. B. Crystal structure of a single α-subunit of the Kv1.2 channel. S1–6 segments, cytoplasmic domain T1, linker connecting the transmembrane portion with the T1 domain (T1–1), as well as N- and C-termini are marked. Charged Arg residues of the membrane voltage sensor S4 are indicated by blue circles. C. Crystal structure of the Kv1.2 channel in a complex with the β-subuni. TM –transmembrane region. D. Gate of the Kv2.1 channel. (140, 150)

1.2.1.2 Expression and characteristics of Kv1.3 and Kv1.5

Kv1.3 was first cloned from brain tissue, and its expression is widely distributed throughout the body (151, 152). it is highly expressed in lymphocytes and the olfactory bulb (153), and it is also expressed in the hippocampus (154), adipose tissue (155), both skeletal and smooth muscle (156-158), epithelia (159) and endothelium (160).

Kv1.3 currents have both characteristic cumulative inactivation and a marked C-type inactivation. The single channel conductance of Kv1.3 is 13 pS and the voltage which is required for activation of Kv1.3 channel is -35 mV (161).

Unlike the Kv1.3 channel, the first site for isolation of Kv1.5 channel was the human ventricle and Kv1.5 is expressed in the atria (162). Like the Kv1.3 channel, Kv1.5 channel is also ubiquitously expressed (151, 152). Kv1.5 is expressed in skeletal and smooth muscle (156-158). Kv1.5 is abundantly expressed in endothelial cells (163) and to a lesser extent in the brain (164, 165).

Kv1.5 currents take part in the ultra-rapid activating K^+ current in the heart known as I_{kur}, which has a role in the repolarization of an action potential (166). The conductance of the Kv1.5 channel is 8 pS and the voltage required for its activation is about 24 mV. In contrast to Kv1.3, the inactivation Kv1.5 is slow and without cumulative inactivation (161).

1.2.1.3 Functions of Kv1.3 and Kv1.5 K+ channels

Kv1.3 and Kv1.5 channels play a role in many cellular processes including maintenance of vascular smooth muscle tone (167), cell growth (168), regulation of cell volume (169) apoptosis (170, 171), adhesion (172), mobility, epithelial transport (173), proliferation (174), insulin release (155) and homeostasis(175).

1.2.1.4 Pharmacology

Kv1.3 and Kv1.5 are inhibited by the general K^+ channel blockers 4-aminopyridine (4-AP) and tetraethylammonium (TEA) (176). Another potent inhibitor for these channels is Psora-4 which has lesser effect on the rest of the Kv isoforms (177). The highly specific toxins such as charybdotoxin and margatoxin (178, 179) and anemone peptide ShK and their derivatives (180) are known to be highly effective for Kv1.3. Kv1.5 is not sensitive to Kv1.3 blockers and has no known specific pharmacology but new chemicals such as S0100176 (from Sanofi-Aventis) (181) or diphenyl phosphine oxide-1 (DPO-1) have been discovered to be potent inhibitors for Kv1.5 (182).

1.2.1.5 Abnormalities

Impaired expression of Kv1.3 in T effector memory cells is involved in the onset of juvenile multiple sclerosis (183). The deficiency of Kv1.3 alters insulin sensitivity and glucose tolerance (184). On the other hand, Kv1.5 loss of function mutations might cause atrial fibrillation (185).

1.3 Inwardly rectifying Kir2.1 Potassium channel

Kir2.1 was the first member of classical Kir channels (Kir2.X) family to be cloned and it has been cloned from a mouse macrophage cell line and named IRK1/Kir2.1/KCNJ2 (186).

It was thought that Kir2.x subunits are made up of homomeric complexes(187). However, it has been shown that Kir2.x subunits can function as heterotetramers in vitro and in vivo. In vitro electrophysiological experiments have revealed that each of Kir2.1, Kir2.2, and Kir2.3 can assemble with any one of the other subunits, and the respective heteromer has different properties from that of their homomers (188).

1.3.1 Structure of Kir2.1

The basic structure of classical Kir channels is composed of transmembrane and cytoplasmic regions and pore structure (189). The inward rectification is due to intracellular ions such as Mg^{2+} (190, 191) and polyamines (192, 193).

Further site-directed mutagenesis recognized negatively charged amino acids (Glu) at two different positions (E224 and E229 for Kir2.1) in the COOH terminus of the cytoplasmic domain that are involved in both Mg^{2+} and polyamine sensitivity (194-197). It has been suggested by Mutagenesis and substituted cysteine accessibility experiments that these residues directly interact with Mg^{2+} and polyamines (198, 199).

The crystal structure of the cytoplasmic domain of Kir2.1 is composed of an intrinsically flexible loop around the membrane face of the cytoplasmic pore (200). The loop narrows the cytoplasmic pore to about 3 A and forms a girdle around the central pore axis. The girdle consists of a loop between βH and βI strands and is known as the G-loop forms the narrowest portion of the ion conduction pathway in the cytoplasmic region. The narrowest part of the G-loop is formed by A306 and to a lesser extent by E299, G300, M301, and M307. A306 is located at the apex of the G-loop. The Charged amino acids, R228, D255, D259, and R260, face the cytoplasmic pore (189, 200).
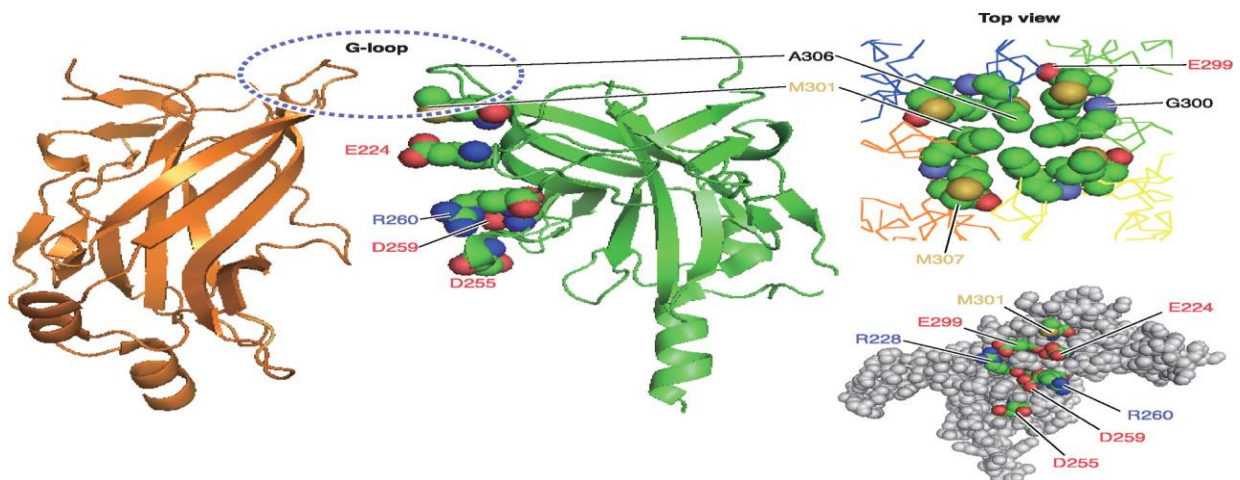
Figure 4: The structure of the cytoplasmic pore region of Kir2.1. Side (left and bottom right) and top-down (top right; membrane to cytoplasm) views of the cytoplasmic region (NH₂ and COOH termini) of the Kir2.1 structure, highlighting amino acids lining the permeation pathway. Cβ atoms (A306) of the G-loop make up the narrowest about 3-Å region of the pore and are shown as open circles for clarity. Other residues near the G-loop are labeled.(189, 200)

1.3.2 Factors regulating the activity of Kir2.1

PKA activators had small effect on Kir2.1 currents (201). The current of Kir2.1 has increased by cAMP when the channel was coexpressed with A kinase-anchoring protein 79 (AKAP79) and treated with the phosphatase inhibitors okadaic acid or cypermethrin (202). Classical Kir channels reconstituted with injection of brain poly(A)$^+$ RNA into *Xenopus* oocytes has been shown to be inhibited by isoproterenol, a β-adrenergic agonist (203). This effect is exerted by the increase of intracellular cAMP and also cGMP (203).

Cytoplasmic regulatory factors such as phosphorylation and pH regulate channel function by affecting the channel-PtdIns(4,5)P₂ interaction. Kir2.1 interacts more strongly with PtdIns(4,5)P₂ (204).

Activity of Kir2.1 on the cell surface can be negatively regulated by its internalization, which is dependent on GTPase Rho family proteins. Kir2.1 expresses a high degree of internalization mediated by dynamin, a protein essential for endocytosis (205, 206).

Other Kir2.1 regulators include arachidonic acid (207), phosphatidylinositol 4,5-bisphosphate PI(4,5)P₂ (208, 209), cholesterol(210), tyrosine kinase phosphorylation(211), TNF-alpha (212), Chapsyn 110 (206) and filamin-A (213),

1.3.3 Overview of Physiological Functions of Kir2.1 in Organs

1.3.3.1 Heart

The classical Kir current I_k is highly expressed in cardiac myocytes, including Purkinje fibers, ventricular and atrial tissues (214-217) but it is absent in nodal cells

(218). I_K play critical role in determining the shape of the cardiac action potential, setting the resting potential, permitting the plateau phase and inducing rapid final stages of repolarization (189). Kir2.1 might be the core subunit that generates the I_K current (219).

1.3.3.2 Blood vessels

Endothelial and smooth muscle cells are the major components of vasculature (189). Electrophysiological studies have shown that classical Kir channels are expressed in both Endothelial and smooth muscle cells (220, 221). Classical Kir channels are the most prominent channels in vascular endothelial cells (221-223). The Functional expression of classical Kir channels provides the driving force for Ca^{2+} influx through Ca^{2+}-permeable channels by seting the E_{res} of endothelial cells to a negative potential. Blockage of endothelial Kir channels by Ba^{2+} inhibits both flow-induced Ca^{2+} influx and vasodilatation caused by Ca^{2+}-dependent production of Nitric Oxide (224, 225).

Kir2.1 was identified in vascular smooth muscle cells but neither Kir2.2 nor Kir2.3 was identified there (226). Blood vessels in Kir2.2 knockout mice dilated normally in response to high extracellular potassium stimulation but not blood vessels from Kir2.1 knockout mice (227). Therefore, Kir2.1 might be the main subunit to which form the classical Kir current in vascular smooth muscle (227).

1.3.3.3 Neurons in the brain

Kir currents were detected in hippocampal neurons (228) and neonatal rat spinal motor neurons (229). The currents which are generated by Kir2.x subunits play an important role in the maintenance of E_{res} and regulation of the excitability of the neurons. Ba^{2+} block of Kir channels in an isolated neuron caused depolarization and initiated the firing of action potential (230).

In situ hybridization histochemistry and immunohistochemistry had showed that that classical Kir channels including Kir2.1 are abundantly and differentially expressed in the whole brain (231).

Kir current has been recorded in Schwann cells surrounding peripheral nerve fibers (232). Kir2.1 and Kir2.3 are expressed in the microvilli of Schwann cells at the nodes of Ranvier (233). As the villi are facing towards the axon, these Kir channels may contribute in maintaining extracellular potassium by absorbing excess K^+ released from excited axons. This function is essential for maintaining proper function of nerve fibers (233).

1.3.3.4 Skeletal muscle

Classical Kir channels play a role in setting the E_{res} and shift it toward the direction of hyperpolarization. Kir2.1 is expressed in skeletal muscle (234). The importance of Kir2.1 in muscle function has been revealed by analysis of Andersen's syndrome. A decrease of the Kir2.1 conductance result in depolarization of the E_{res}, leading to inactivatation of Na^+ channels and thus prevent initiation and propagation of action potentials (235).

The functional expression of Kir2.1 is necessary for differentiation of myoblasts (236) and for the fusion of mononucleated myoblasts to form a multinucleated skeletal muscle fiber (237). Kir2.1 induce hyperpolarization which maintain the membrane potential in a range where Ca^{2+} can enter the myoblasts through Ca^{2+} permeable channels promoting the differentiation and fusion of myoblasts (237).

1.3.3.5 KIDNEY

Kir2.1 is found in juxtaglomerular cells and it is not found in epithelial cells or glomeruli (238). Kir2.1 plays a major role in setting the membrane potential in the juxtaglomerular cells (238).

Activation of Kir2.1 in proximal renal tubules increases the electrical driving force for electrogenic bicarbonate exit across the basolateral cell membrane leading to cytosolic acidification and subsequent stimulation of the apical Na^+/H^+ exchanger and thus increases Na^+ entry And the demand for Na^+ extrusion through the Na^+/K^+ ATPase (239).

1.3.4 Abnormalities

1.3.4.1 Andersen's Syndrome (LQT type7)

Andersen's syndrome is characterized by cardiac arrhythmias of long Q-T syndrome (LQT7), dysmorphic bone structure in the face and fingers and periodic paralysis (240). It is an autosomal dominant disorder due to loss of function mutations in the KCNJ2 gene which encodes the Kir2.1 subunit (235). These mutations induce dominant negative effects on the K^+ current (241, 242) by impairing the interaction between the channels and $PtdIns(4,5)P_2$ (243) or by inhibiting trafficking of Kir2.1 to cell membrane surface (241). Cardiac Arrhythmias in Andersen's syndrome is due to reduction of Kir2.1 function that prolongs the plateau phase of the action potential and depolarizes the resting membrane potential. Abnormal bone structure can be caused by the dysfunction of osteoclasts. Since the Low extracellular pH in the extracellular matrix is maintained by H^+ secretion by a proton pump is critical for proper functioning of the osteoclasts and as this H^+ secretion is achieved in exchange for K^+ transport through Kir2.1 channels, disruption of Kir2.1 channels can cause osteoclast dysfunction which can lead to severe bone deformity(189).

1.3.4.2 Short Q-T syndrome

The short Q-T syndrome which is associated with a high incidence of sudden cardiac death, syncope, and/or atrial fibrillation even among newborns and young patients due to gain of function mutation affecting the Kir2.1 gene (244).

1.4 Aim of the study

B19V infection is common in humans (245). B19V infection is associated with myocarditis (246, 247). Endothelial B19V infection may lead to isolated left ventricular diastolic dysfunction (76) and B19V associated myocarditis thus causing an endothelial cell mediated disease (248). In pregnancy B19V-infection may be followed by maternal and fetal myocarditis, congenital malformations, stillbirth and abortion (78-81). B19V preferably invades into proliferating cells thus causing particularly severe disorders during antenatal infection (82). Endothelial rather than myocardial B19V genomes were detected in fatal inflammatory cardiomyopathy (33, 34).

The B19V genome encodes the structural capsid proteins VP1 (6) VP1 contains a sequence homologous to the catalytic site and Ca^{2+}-binding loop of secreted phospholipase A2 (sPLA2) (21-23). The vPLA2 enzyme activity is disrupted by replacement of a histidine at position 153 with alanine ([H153A]VP1) (23, 24). Expression of VP1 but not of [H153A]VP1 in endothelial cells upregulates Ca^{2+} entry (249), an effect mimicked by PLA2 product lysophosphatidylcholine (249). VP1 has further been shown to inhibit Na^+/K^+ ATPase activity (250), an effect abrogated by loss of function mutation of the PLA2 sequence and mimicked by lysophosphatidylcholine (250, 251).

The aim of present study is to explore whether expression of VP1 influences the activity of the Potassium channels Kv1.3 and Kv1.5, which are expressed in the endothelium (160, 163) and are critically important for proliferation in several cell types (252, 253) and whether expression of VP1 influences the activity of the inwardly rectifying Kir2.1 K^+ channels, which have previously been shown to be expressed in endothelial cells (221). Moreover, to explore whether the effect of VP1 on Kv1.3, Kv1.5 and Kir2.1 Potassium channels is sensitive to inhibition of PLA2 and is mimicked by lysophosphatidylcholine.

2. Material

2.1. Two electrode voltage clamp

2.1.1. Technical equipments

Name	manufacturer and country of origin
Autoclave HICCAVE-50 HMC	System labor systemtechnik, Wettenberg, Germany.
Digitizer digidata 1322A	Axon Instruments, Union City, CA, USA
DMZ universal puller	Zeitz-instruments, Martinsried. Germany.
Eppendorf centrifuge 5415R	Hinz gmdh. Hamburg. Germany
Eppendorf pipettes 0.1-1000ul	Eppendorf. Hamburg. Germany.
Gene clamp 500 amplifier	Axon Instruments, Union City, CA, USA
Maclab D/A converter	AD instruments, Castle Hill, Australia.
Nanoliter injector 2000	World precision instruments, Berlin, Germany.
pH meter 646	Carl Zeiss, Oberkochen. Germany
Safety cabinet class II(Hera safe)	Kendro laboratory products, Langenselbold, Germany

2.1.2 Stock materials

Name	manufacturer and country of origin
Borosilicate glass capillaries (injection) (External diameter: 1.14mm, internal diameter: 0.5mm)	Harvard apparatus, USA
Borosilicate glass capillaries (measurement) (External diameter: 1.5mm, internal diameter: 1.17mm)	Harvard apparatus, USA.
Milipore express plus high flow rate membranes (PES). 73mm/0.22um.	Milipore, Schwalbach, Germany.
Combitips plus 2.5 ml	Eppendorf, Hamburg, Germany

| Eppendorf tubes | Eppendorf, Hamburg, Germany |
| Falcon tubes (50ml) | Greiner bio-one, Frickenhausen, Germany |

2.1.3 Software

Name	manufacturer and country of origin
Microsoft office 2002 SP3	Microsoft corp. Redmond, USA.
Microcal Origin 6.0G	Microcal software, Northampton, MA, USA.
GraphPad InStat v3.05	GraphPad Software Inc., La Jolla, CA, USA
pClamp 9.0 software package	Axon Instruments, Union City, CA, USA.
MacPyMOL 1.3 (Open source)	DeLano Scientific, Schödinger, LLC. USA.

2.1.4 Chemicals

Name	Manufacturer and country of origin
Acetone	Sigma-Aldrich Chemie GmbH, Steinheim, Germany.
$CaCl_2 \times 2H_2O$	Sigma-Aldrich Chemie GmbH, Steinheim, Germany.
Collagenase Type II	Worthington Biochemical Corp., NJ, USA.
HEPES	Carl Roth GmbH, Karlsruhe, Germany.
KCl	Carl Roth GmbH, Karlsruhe, Germany.
Methanol	Sigma-Aldrich Chemie GmbH, Steinheim, Germany.
$MgCl_2 \times 6H_2O$	Sigma-Aldrich Chemie GmbH, Steinheim, Germany.
NaCl	Sigma-Aldrich Chemie GmbH, Steinheim, Germany.
Paraffin	Merck, Darmstadt, Germany.
Sodium pyruvate	Sigma-Aldrich Chemie GmbH, Steinheim, Germany.
Theophylin (Euphylon ©)	Nycomed GmdH, Konstanz, Germany.
Phenphormin hydrochloride	Sigma-Aldrich Chemie GmbH, Steinheim, Germany.
Tetracycline	Sigma-Aldrich Chemie GmbH, Steinheim, Germany.

Ciprofloxacin	Fresenius Kabi Austria GmdH, Austria.	
Gentamycinsultaf (Refobacin ©)	Merck Serono, Dramstadt, Germany.	
Actinomycin D	Sigma-Aldrich Chemie GmbH, Steinheim, Germany.	
L-α-Lysophosphatidylcholine	Sigma-Aldrich Chemie GmbH, Steinheim, Germany.	
Ouabain Octahydrate	Calbiochem, Darmstadt, Germany.	

2.1.5 Solutions

	ND96	ND96-A	OR2	OR2-Collagenase
NaCl	96	88.5	82.5	82.5
KCl	2	2	2	2
CaCl.2H2O	1.8	1.8		
MgCl2.6H2O	1	1	1	1
HEPES	5	5	5	5
Sodium pyruvate		5		
Tetracyclin		0.11		
Ciprofloxacin		0.004		
Refobacin		0.222		
Theophylin		0.498		
Collagenase				2 mg/ml
pH	7.4	7.5	7.4	7.4

Table 1: Composition of solutions used for two-electrode voltage clamp experiments (in mM unless stated otherwise)

3. Methods

3.1 Preparation of cRNA

B19V DNA was isolated from deparaffinized myocardial tissue of a patient with fatal B19V-associated inflammatory cardiomyopathy after proteinase K digestion, phenol/chloroform extraction and ethanol precipitation (accession number: DQ225150). Constructs encoding wild-type VP1 (250), PLA2-negative ^{H153A}VP1 mutant (250), mouse Kv1.5 (254), mouse Kv1.3 (255) wild-type Kir2.1 (256) were used for generation of cRNA

The cRNA synthesis protocol consists of two steps:
1. Linearization of the plasmid DNA containing the sequence of interest.
2. Generation of cRNA itself.

3.1.1 Plasmid DNA linearization
Endonucleases were used to obtain a cut at the 3' end of the insert. Specific restriction enzymes as shown in table 2 were used to linearize specific plasmids.

Table 2: Plasmids containing the desired genes encoding for specific proteins and restriction endonuclease enzymes used to linearize each plasmid.

Protein	Plasmid	Restriction Endonuclease
Kv1.3	pSP64T	EcoR I
Kv1.5	pBluescript SK	BamH I
Kir2.1	pGHJ	Mlu I

VP1	pGHJ	Xba I
^{H153A}VP1	pGHJ	Xba I

The reaction mixture as presented in the table below was prepared and incubated overnight at 37°C. Afterwards DNA was purified by NucleoSpin® Gel and PCR clean-up: a 250 µl NTI Buffer was added to the reaction mixture and loaded in a NucleoSpin® Gel and PCR clean-up column that was centrifuged at 11000 rpm for 30 seconds. The column was washed twice with a 700 µl NT3 Buffer and centrifuged at 11000 rpm for 1 minute. After centrifugation DNA was eluted with a 20 µl NE Buffer. Then cRNA concentration was measured by taking 1 µl of cRNA in 69µl water using an Eppendorf Biophotometer (Hamburg, Germany). Finally, to confirm quality of generated cRNA its quality was checked by gel electrophoresis.

Table 3: Reaction mixture used to linearize DNA plasmid

Reaction mixture	Quantity
10 X Buffer	5 µl
Plasmid DNA (10 µg)	Depends on DNA concentration
Restriction enzyme (20 U)	2 µl
Water	Fill till reach a total volume of 25 µl

3.1.2 cRNA synthesis

The linearized DNA produced by the method mentioned above was used as a template to generate cRNA. The reaction mixture listed below was put in a sterile eppendorf tube.

Table 4: Reaction mixture used to synthesize RNA from the linearized DNA.

Reaction mixture	Quantity
10 X Buffer	2.5 µl
rNTPs	1 µl
Cap analog	2.5 µl
RNAse inhibitor	1 µl
Water	Fill till reach a total volume of 25 µl

The reaction mixture was gently spun and the appropriate RNA polymerase was added and spun again. RNA polymerases T7 or T3 or Sp6 were used, and the mixture was then incubated at 37°C for 2 hours, 5 µl of DNAse was added in the reaction mixture afterwards to remove the possible DNA contamination. Finally the reaction mixture was incubated at 37°C for 15 minutes under continuous shaking.

Table 5: RNA polymerases used to prepare cRNA and amount of cRNA injected into oocytes.

Protein	RNA polymerase	cRNA (ng/oocytes)	Exp. time (days)
Kv1.3	Sp6	2.5 ng	3
Kv1.5	T3	2.5 ng	3
Kir2.1	T7	10 ng	3
VP1	T7	10 ng	3

H153AVP1	T7	10 ng	3

To purify the generated RNA, 129 µl of phenol chloroform mixture was mixed with 100µl of DEPC water and was added in an eppendorf and centrifuged at 11000 rpm for 5 minutes. After that, the upper inorganic phase was carefully taken into a new eppendorf tube, 12.5 µl of 3 M sodium acetate (pH 5.2) was added, as well as 375 µl of 100% ethanol and then mixed and further incubated at -70°C for at least 30 minutes.

After incubation, the mixture was centrifuged at 20000 rpm for 15 minutes at 4°C. The supernatant was removed and the pellet was washed with 500 µl of 70% ethanol. Finally the pellet was left to dry in a dryer machine for 5 minutes and reconstituted in 40 µl of DEPC water and mixed again. Then cRNA concentration was measured by taking 1 µl of cRNA in 69 µl water using an Eppendorf Biophotometer (Hamburg, Germany). Finally, to confirm the quality of generated cRNA its quality was checked by gel electrophoresis. All the cRNA was provided by the department of Molecular Biology.

3.2 *Xenopus Laevis* oocyte preperation

The *Xenopus Laevis* female frog was anesthetized by immersion in a solution containing 0.1% ethyl 3-aminobenzoate methanesulfonate salt (Tricain) before the operation and the frogs was laid during operation on an absorbent paper coated with the solution in order to increase the duration of the effect of the Tricain.

A small longitudinal incision (around 1-2 cm) was made in the lower abdomen for careful cutting of several pieces of the ovarian lobes and then the oocyte bags were extracted into small portions to avoid contamination through the *Xenopus* skin. Surgical blanket was placed at the operation incision and all the surgical instruments were properly sterilized as a protective measure.

The oocyte bags were put in a Petri dish containing the calcium free solution (OR2) for further separation, cleaning and preparation. The incision was cleaned properly and closed with reabsorbant stitches. The internal tissues mainly muscles and the external tissues (skin) were closed separately to aid the healing process.

The *Xenopus laevis* frog was taken back to a provisional cage and was washed several times to be cleaned from possible traces of residual anaesthesia. After 30 minutes of continuous washing when the frog recovered its reflexes and movement, it was washed two additional times. The frog was returned to the aquarium after the total recovery of its reflexes.

The oocyte bags were extracted manually and divided into smaller groups to facilitate their digestion by the collagenase. The collagenase solution was prepared at a concentration of 2 mg/ml in OR2 and the oocytes were placed in a 50 ml Falcon tube containg collagenase recoated by aluminium foil to avoid external light interference. The duration of the digestion process was about 2-3 hours, depending of the digestion procedure, the frog, or the times that this frog was already operated. After the second hour of digestion, the oocytes were periodically visualized under the microscope every 30 minutes to check the status of the oocytes and to avoid excessive digestion by the collagenase. When the oocytes were determined to be ready for selection and injection, they were washed twice with OR2 and then with the ND-96 with antibiotics solution (ND96-A).The oocytes were then stored in a petri dish containing 3-3.5 ml of ND96-A. These stored oocytes can survive till 5-6 days if the petri dish containing the oocytes is kept in an incubator at a temperature of 17° C and the dead cells are removed and the media is changed periodically. The oocytes in growing stage V-VI, with a clear differentiation between poles, were selected for further experiments. All the cRNA injections were done at the same day of the operation.

The cRNA injections were done with a Nanoinjector 2000, previously configured for the suitable volume. A manually prepared borosilicate capillary was used for cRNA injection. After cutting the capillary edge and allowing a diameter of about 10-20 μm at the end, the capillary was manually filled with paraffin oil and afterwards inserted into the microinjector. Careful attention was made all the time to avoid accidental contamination by cleaning the working place, using sterile pipettes, gloves, and DEPC water to dilute stock cRNA preparations. Oocytes injected with cRNA were stored in Petri dishes containing 3 -3.5 ml of sterilized ND96-A solution in an incubator at a temperature of 17° C for 3 days until having considerable expression of the injected cRNA.

3.3 Potassium channels current recording in Xenopus laevis oocytes with Two electrode voltage clamp (TEVC)

Two electrode voltage clamp (TEVC) is an important electrophysiological technique which depends on clamping the membrane potential of Xenopus Laevis oocytes to several voltage steps or fixing it to one holding potential in order to measure and record the charged particles movement across the membrane through ion channels, electrogenic transporters or pumps which were heterologously expressed in the plasma membrane of Xenopus oocytes.
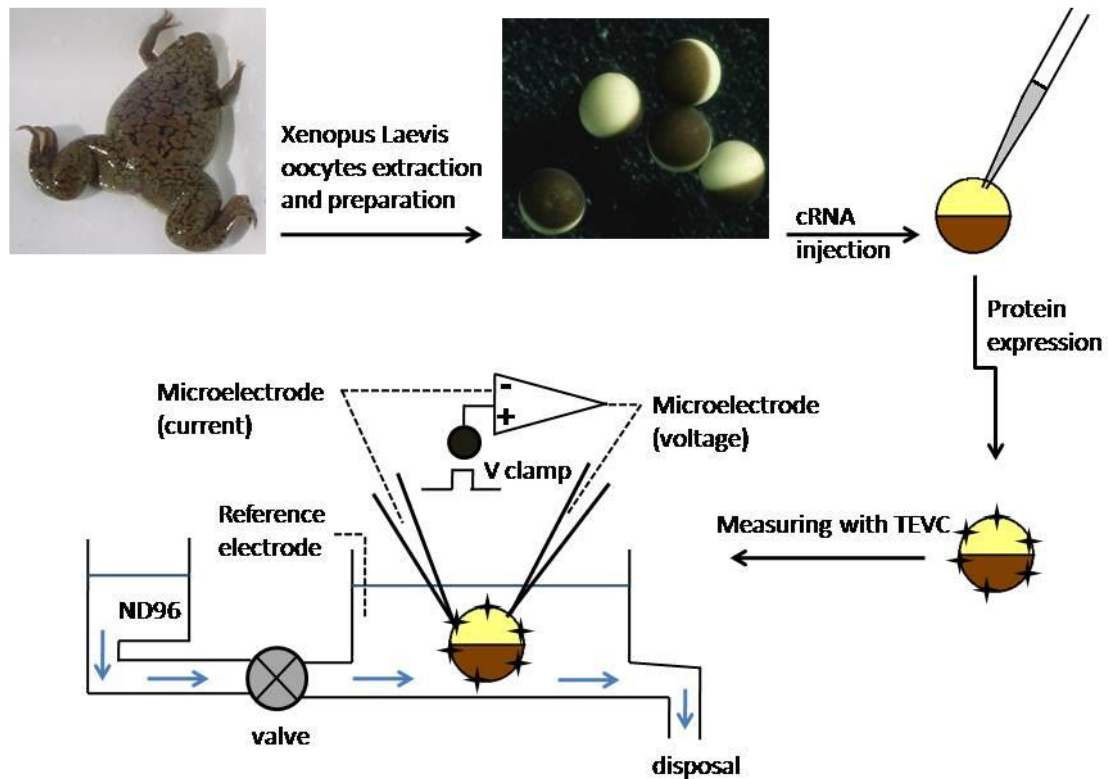
Figure 5: An illustrative scheme for steps needed to measure with the two electrode voltage clamp technique (TEVC) in Xenopus oocytes.

The two electrode voltage clamp measurement is achieved by introducing two glass microelectrodes inside the oocyte to reach the intracellular compartment. The first electrode records the membrane potential and the second electrode is the current injecting electrode. The signal recorded by the recording electrode reaches a feedback amplifier to compare it to the voltage clamp command set by a generator. The difference between these two signals is injected forward through the current injecting electrode to the intracellular leaflet of the Xenopus Laevis oocytes and back through the cell membrane to the reference electrode to complete the circuit. The deflection from the baseline is quantified and visualized as an electrogenic activity of the ion channels, transporters or pumps. The

reference electrodes are made of silver and coated with a silver chloride (AgCl) coating, whereas the microelectrodes are filled with KCl (3M) and connected to the feedback amplifier. The setup is covered by Grounded Faraday cage to prevent against possible external noise currents. Vibration and mechanical noise are reduced by using Pneumatic anti-vibration stage. The electrode potential was set to 0 mV after immersion in the bath solution and just before introducing the electrodes inside the oocytes. Under low magnification stereomicroscope (5-20X), oocytes were impaled with glass capillaries at opposite poles using micromanipulators.

For Kv1.3 and Kv1.5 experiments, *Xenopus* oocytes were prepared as previously described (257), cRNA encoding Kv1.3 (2.5ng) or Kv1.5 (2.5ng), VP1 (10 ng) and ^{H153A}VP1(10ng) was injected on the same day of preparation of the *Xenopus* oocytes. All experiments were performed at room temperature (about 22° C) 3 days after the injection (258, 259). Two-electrode voltage clamp recordings were performed at a holding potential of -100 mV. The currents were recorded following 2 second depolarizing pulses ranging from −80 to +50 mV in 10-mV and 15-s or 20-s increments from a holding potential of −100 mV. The data were filtered at 1 kHz and recorded with a Digidata 1322A A/D-D/A converter and ClampexV .9.2 software for data acquisition (Axon Instruments). The analysis of the data was performed with Clampfit 9.2 (Axon Instruments) software (260, 261). The oocytes were maintained at 17°C in ND96-A solution. The control superfusate (ND96) contained 96 mM NaCl, 2 mM KCl, 1.8 mM $CaCl_2$,1 mM $MgCl_2$ and 5 mM HEPES, pH was adjusted to 7.4 by addition of NaOH (262). The flow rate of the superfusion was 20 ml/min, and a complete exchange of the bath solution was reached within about 10 s (263, 264).

To investigate whether the effect of VP1 on Kv1.3 or Kv1.5 is modified by actinomycin, Kv1.3 or Kv1.5 was expressed in *Xenopus* oocytes with additional

expression of VP1 in the presence of actinomycin (10 µM, added 36 hours prior to the experiment).

To investigate whether Lysophosphatidylcholine affect the activity of Kv1.3 and Kv1.5 K channels, *Xenopus* oocytes expressing Kv1.3 or Kv1.5 were treated with lysophosphatidylcholine (1µg/ml) for 10 minutes.

For Kir2.1 experiments, *Xenopus* oocytes were prepared as previously described (257, 265). cRNA encoding Kir2.1(10ng), VP1 (10 ng) and [H153A]VP1(10ng) was injected on the same day of preparation of the *Xenopus* oocytes (266, 267). All experiments were performed at room temperature (about 22° C) 3 days after the injection (268). In two-electrode voltage clamp experiments Kir2.1 currents were elicited every 20 s with 1 s pulses from -150 mV to +30 mV applied from a holding potential of -60 mV. The data were filtered at 1 kHz and recorded with a Digidata 1322A A/D-D/A converter and ClampexV.9.2 software for data acquisition (Axon Instruments) (269, 270). The analysis of the data was performed with Clampfit 9.2 (Axon Instruments) software (271, 272). The oocytes were maintained at 17°C in ND96-A solution. The control superfusate (ND96) contained 96 mM NaCl, 5 mM KCl, 1.8 mM $CaCl_2$,1 mM $MgCl_2$ and 5 mM HEPES, pH was adjusted to 7.4 by addition of NaOH (256). The flow rate of the superfusion was 20 ml/min, and a complete exchange of the bath solution was reached within about 10 s (273, 274).

To test whether Lysophosphatidylcholine affect the activity of Kir2.1 K+ channels, *Xenopus* oocytes expressing Kir2.1 were treated with lysophosphatidylcholine (1µg/ml) for 10 minutes.

To test whether the effect of VP1 expression or lysophosphatidylcholine treatment could be mimicked by inhibition of the Na^+/K^+ ATPase with Ouabain. Kir2.1 expressing oocytes were treated with Ouabain (0.1 mM) for 10 minutes.

To test whether the inhibition of Na^+/K^+ ATPase was required for the inhibitory effect of lysophosphatidylcholine on Kir2.1. The Kir2.1 expressing oocytes were treated either with lysophosphatidylcholine (1µg/ml) alone or with both lysophosphatidylcholine (1µg/ml) and Ouabain (0.1 mM) for 10 minutes.

3.4 Statistical analysis

Data are provided as means ± SEM, n represents the number of oocytes investigated. All experiments were repeated with at least 3 batches of oocytes; in all repetitions qualitatively similar data were obtained. Data were tested for significance using analysis of variance (ANOVA) or t-test, as appropriate. Results with $p < 0.05$ were considered statistically significant.

4. Results

4.1 Regulation of Kv1.3 by VP1

4.1.1 Inhibition of Kv1.3 currents in Kv1.3 expressing *Xenopus* oocytes by coexpression of VP1 but not of [H153A]VP1

The present study explored the impact of parvovirus B19 capsid protein VP1 on Kv1.3 K^+-channel activity. In order to test whether VP1 regulate the Kv1.3 K^+ current, Kv1.3 was expressed in *Xenopus* oocytes with or without additional expression of VP1 or the [H153A]VP1 mutant lacking functional PLA2 activity. K^+ peak currents taken as a measure of K^+ channel activity.
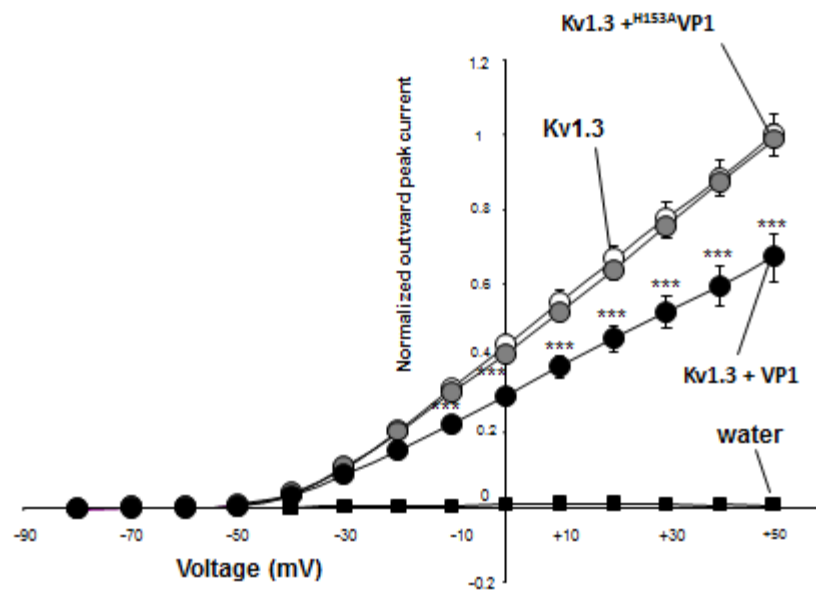
Figure 6: normalized I/V curve of Kv1.3 K$^+$ current with and without Coexpression of VP1 or the PLA2-negative ^{H153A}VP1 mutant

Arithmetic means ± SEM (n =9-24) of the normalized depolarization-induced Kv1.3 peak current as a function of voltage in *Xenopus* oocytes injected with water (black squares), or with cRNA encoding Kv1.3 alone (white circles) or with cRNA encoding both, Kv1.3 and VP1 (black circles) or with cRNA encoding Kv1.3 and PLA2-negative VP1 mutant (grey circles). Peak currents were normalized to the mean peak current at +50 mV in *Xenopus* oocytes injected with cRNA encoding Kv1.3. *** (p<0.001) indicates statistically significant difference from *Xenopus* oocytes injected with cRNA encoding Kv1.3 (separated unpaired student t test).
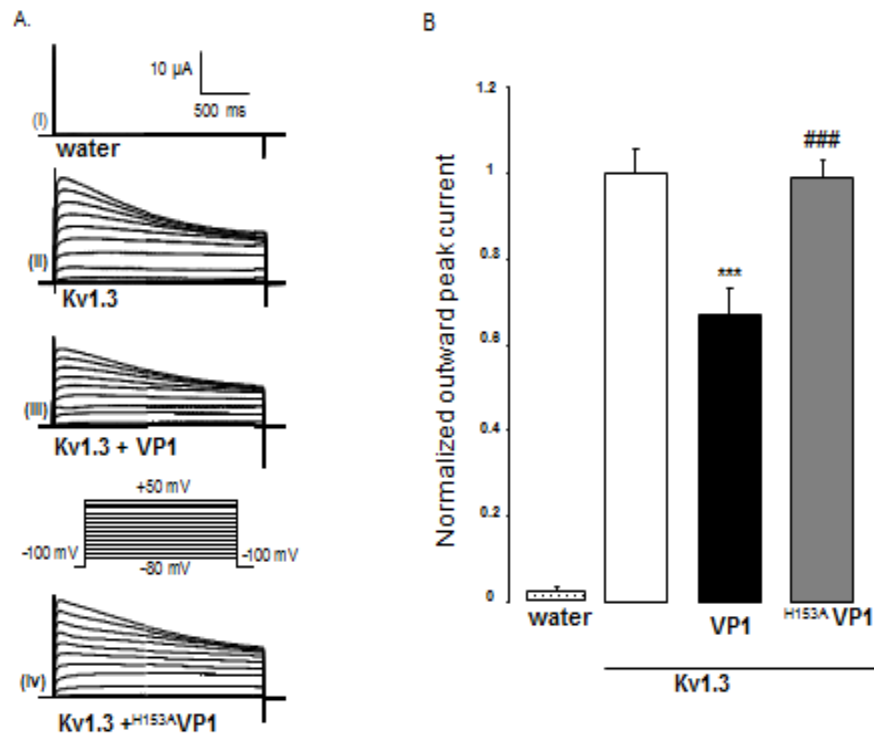
Figure 7: effect of VP1 co-expression on K$^+$ currect in Kv1.3 expressing Xenopus oocytes

A.Original tracings recorded in *Xenopus* oocytes injected with water (i), with cRNA encoding Kv1.3 alone (ii) with cRNAs encoding both, Kv1.3 and VP1 (iii) and with cRNA encoding both, Kv1.3 and the PLA2-negative [H153A]VP1 mutant (iv). The currents were recorded following 2 second depolarizing pulses ranging from −80 to +50 mV in 10 mV and 15 second increments from a holding potential of −100 mV.**B.**Arithmetic means ± SEM (n = 9-24) of the normalized Kv1.3 peak current at +50 mV in *Xenopus* oocytes injected with water (dotted bar), with cRNA encoding Kv1.3 alone (white bar) with cRNA encoding both, Kv1.3 and VP1 (black bar) or with cRNA encoding Kv1.3 and PLA2-negative VP1 mutant (grey bar). *** indicates statistically significant (p<0.001) difference from *Xenopus* oocytes injected with cRNA encoding Kv1.3 (ANOVA-one way).

As shown in Figure 7, K$^+$ current was low in *Xenopus* oocytes injected with water. Expression of Kv1.3 resulted in a strong current, which was significantly decreased by coexpression of VP1. In contrast, coexpression of the [H153A]VP1 mutant lacking PLA2 activity did not significantly modify Kv1.3 currents. As a result, in Kv1.3 expressing *Xenopus* oocytes the K$^+$ current was significantly higher following coexpression of [H153A]VP1 than following coexpression of VP1

4.1.2   Inhibition of K$^+$-current in Kv1.3 expressing *Xenopus* oocytes by VP1 Co-expression in presence of D-actinomycin

In order to test, whether the effect of VP1 required transcription, additional experiment was performed in the presence of actinomycin (10 µM, added 36 hours prior to the experiment), Kv1.3 was expressed in Xenopus oocytes with additional expression of VP1 in the presence of actinomycin
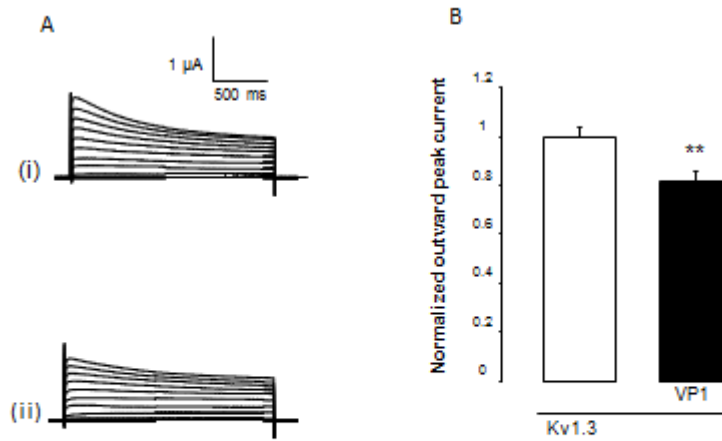
Figure 8: effect of VP1 co-expression on currect in Kv1.3 expressing Xenopus oocytes in the presence of D-Actinomycin

A. Original tracings recorded in oocytes injected with cRNA encoding Kv1.3 alone (i) or with cRNA encoding both, VP1 and Kv1.3 (ii), each with prior 36 hours treatment with 10 µM D-actinomycin. The currents were recorded following 2s depolarizing pulses ranging from −80 to +50 mV in 10 mV and 15 s increments from a holding potential of −100 mV.

B. Arithmetic means ± SEM (n = 19-20) of the normalized K^+-peak current following a depolarization from −80 to +50 mV in oocytes injected with cRNA encoding Kv1.3 alone with prior 36 hours treatment with 10 µM D-actinomycin (white bar) or with cRNA encoding both, VP1and Kv1.3 (black bar), each with prior 36 hours treatment with 10 µM D-actinomycin. ** indicates statistically significant ($p < 0.01$) difference from absence of VP1 (unpaired student t-test).

As shown in Figure 8, even in the presence of actinomycin (10 µM, added 36 hours prior to the experiment) the coexpression of VP1 with Kv1.3 decreased the K^+ current in Kv1.3 expressing oocytes. Thus, the effect of VP1 on Kv1.3 did not require transcription.

4.1.3 Inhibition of K$^+$-channel activity in Kv1.3 expressing *Xenopus* oocytes by lysophosphatidylcholine

Phospholipase A2 (PLA2) of VP1 is known to generate lysophosphatidylcholine. Thus, additional experiment was performed to explore whether lysophosphatidylcholine influences K$^+$ currents in Kv1.3 expressing Xenopus oocytes, Kv1.3 expressing oocytes were treated with lysophosphatidylcholine(1µg/ml) for 10 minutes
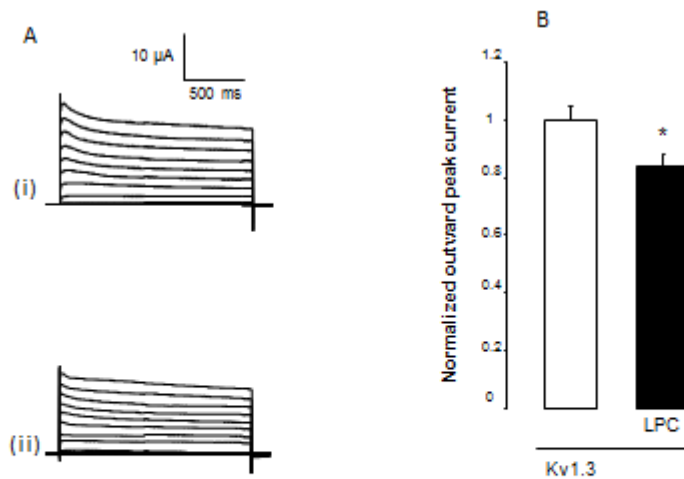
Figure 9: effect of Lysophosphatidylcholine on K$^+$ currect in Kv1.3 expressing Xenopus oocytes

A. Original tracings recorded in oocytes injected with cRNA encoding Kv1.3 alone in the absence (i) or presence (ii) of lysophosphatidylcholine (1 µg/ml). The currents were recorded following 2s depolarizing pulses ranging from −80 to +50 mV in 10mV and 15 s increments from a holding potential of −100 mV.

B. Arithmetic means ± SEM (n = 16) of the normalized K$^+$-peak current following a depolarization from -80 mV to +50 mV in oocytes injected with cRNA encoding Kv1.3 alone in the absence (white bar) and presence (black bar) of lysophosphatidylcholine (1 µg/ml). * indicates statistically significant (p<0.05) difference from absence of lysophosphatidylcholine (unpaired student t test).

As shown in Figure 9, treatment of Kv1.3 expressing *Xenopus* oocytes with lysophosphatidylcholine (1µg/ml) for 10 minutes was indeed followed by a decrease of K^+ currents.

4.2 Regulation of Kv1.5 by VP1

4.2.1 Inhibition of Kv1.5 K^+ currents in Kv1.5 expressing *Xenopus* oocytes by coexpression of VP1 but not of [H153A]VP1

The second part of study explored the impact of the parvovirus B19 capsid protein VP1 on Kv1.5 K^+ channel activity. In order to test whether VP1 regulate the Kv1.5 K^+ current, Kv1.5 was expressed in *Xenopus* oocytes with or without additional expression of VP1 or the [H153A]VP1 mutant lacking functional PLA2 activity. K^+-peak currents taken as a measure of K^+ channel activity
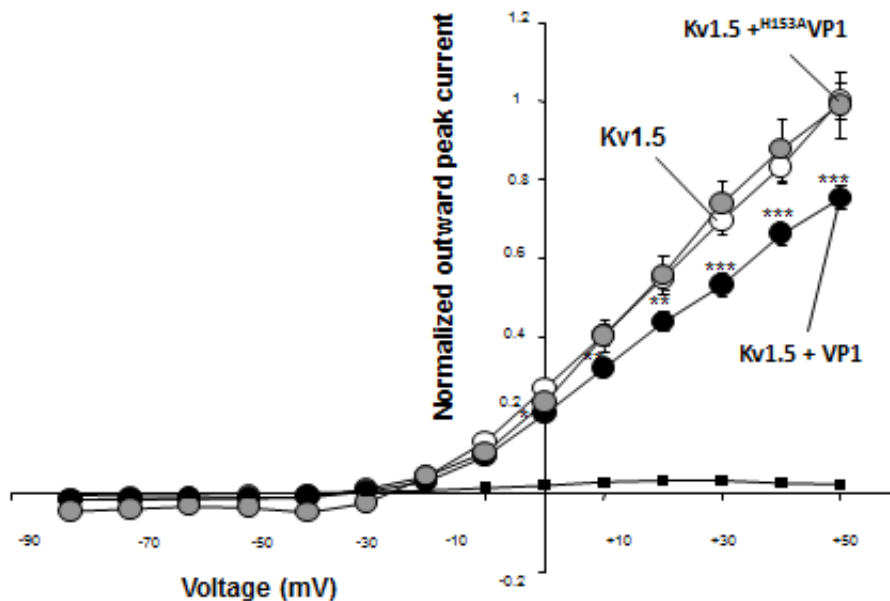
Figure 10: normalized I/V curve of KV1.5 K$^+$ current with and without Coexpression of VP1 or the PLA2-negative ^{H153A}VP1 mutant

Arithmetic means ± SEM (n =3-26) of the normalized depolarization induced Kv1.5 peak current as a function of voltage in *Xenopus* oocytes injected with water (black squares), or with cRNA encoding Kv1.5 alone (white circles) or with cRNA encoding both, Kv1.5 and VP1 (black circles) or with cRNA encoding Kv1.5 and PLA2-negative VP1 mutant (grey circles). Peak currents were normalized to the mean peak current at +50 mV in *Xenopus* oocytes injected with cRNA encoding Kv1.5. *** (p<0.001) indicates statistically significant difference from *Xenopus* oocytes injected with cRNA encoding Kv1.5 (separated unpaired student t tests).
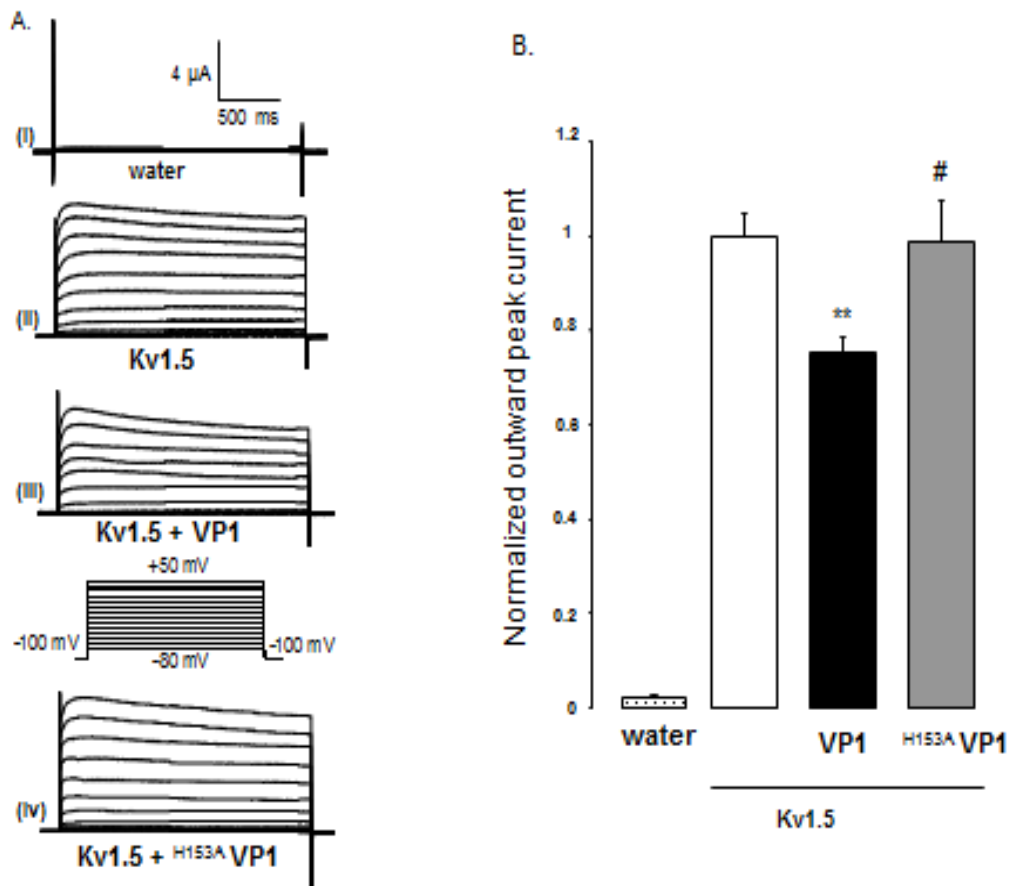
Figure 11: effect of VP1 co-expression on K$^+$ currect in Kv1.5 expressing Xenopus oocytes

A.Original tracings recorded in oocytes injected with water (i), with cRNA encoding Kv1.5 alone (ii) with cRNAs encoding both, Kv1.5 and VP1 (iii) and with cRNA encoding both, Kv1.5 and the PLA2-negative ^{H153A}VP1 mutant (iv). The currents were recorded following 2 second depolarizing pulses ranging from −80 to +50 mV in 10 mV and 20 second increments from a holding potential of −100 mV.**B.**Arithmetic means ± SEM (n =3-26) of the normalized Kv1.5 -peak current at +50 mV in *Xenopus* oocytes injected with water (dotted bar), with cRNA encoding Kv1.5 alone (white bar) with cRNA encoding both, Kv1.5 and VP1 (black bar) and with cRNA encoding both, Kv1.5 and PLA2-negative VP1 mutant (grey bar). ** indicates statistically significant (p<0.01) difference from *Xenopus* oocytes injected with cRNA encoding Kv1.5 (ANOVA-one way).

As shown in Figure 11, The K$^+$ current in *Xenopus* oocytes expressing Kv1.5 was significantly decreased by coexpression of VP1. Coexpression of the ^{H153A}VP1 mutant lacking PLA2 activity did not significantly modify Kv1.5 currents. The K$^+$ current in Kv1.5 expressing *Xenopus* oocytes was thus significantly higher following coexpression of ^{H153A}VP1 than following coexpression of VP1.

4.2.2 Inhibition of K$^+$ current in Kv1.5 expressing *Xenopus* oocytes by VP1 coexpression in presence of D-actinomycin

In order to test, whether the effect of VP1 required transcription, additional experiments were performed in the presence of actinomycin (10 μM, added 36 hours prior to the experiment). Kv1.5 was expressed in xenopus oocytes with additional expression of VP1 in the presence of actinomycin.
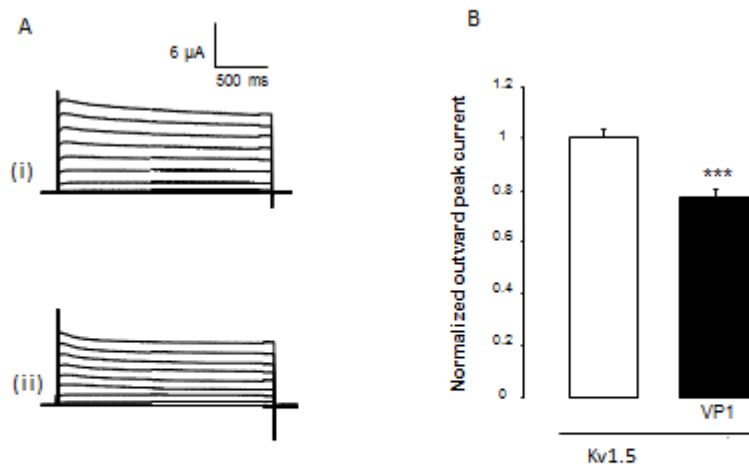
Figure 12: effect of VP1 co-expression on currect in Kv1.5 expressing Xenopus oocytes in the presence of D-Actinomycin

A. Original tracings recorded in oocytes injected with cRNA encoding Kv1.5 alone (i) or with cRNA encoding both, VP1 and Kv1.5 (ii), each with prior 36 hours treatment with 10 µM D-actinomycin. The currents were recorded following 2s depolarizing pulses ranging from −80 to +50 mV in 10mV and 20 s increments from a holding potential of −100 mV.

B. Arithmetic means ± SEM (n = 18) of the normalized K^+-peak current following a depolarization from -80 mV to +50 mV in oocytes injected with cRNA encoding Kv1.5 alone (white bar) or with cRNA encoding both,Kv1.5 and VP1 (black bar), each with prior 36 hours treatment with 10 µM D-actinomycin. *** indicates statistically significant (p<0.001) difference from absence of VP1 (unpaired student t- test).

As shown in Figure 12, even in the presence of actinomycin (10 µM, added 36 hours prior to the experiment), the coexpression of VP1 decreased the K^+ current in Kv1.5 expressing oocytes. Thus, the effect of VP1 on Kv1.5 did not require transcription.

4.2.3 Inhibition of K⁺channel activity in Kv1.5 expressing *Xenopus* oocytes by lysophosphatidylcholine

PLA2 of VP1 is known to generate lysophosphatidylcholine. Thus, additional experiments were performed to test whether lysophosphatidylcholine influences K^+ currents in Kv1.5 expressing Xenopus oocytes. Kv1.5 expressing oocytes were treated with lysophosphatidylcholine (1µg/ml) for 10 minutes.

Figure 13: effect of Lysophosphatidylcholine on K⁺ currect in Kv1.5 expressing Xenopus oocytes

A. Original tracings recorded in oocytes injected with cRNA encoding Kv1.5 alone in the absence (i) or presence (ii) of lysophosphatidylcholine (1 µg/ml). The currents were recorded following 2s depolarizing pulses ranging from −80 to +50 mV in 10mV and 20 s increments from a holding potential of −100 mV.

B. Arithmetic means ± SEM (n = 14-16) of the normalized K^+-peak current following a depolarization from -80 mV to +50 mV in oocytes injected with cRNA encoding Kv1.5 alone in the absence (white bar) and presence (black bar) of lysophosphatidylcholine (1 μg/ml). ** indicates statistically significant (p<0.01) difference from absence of lysophosphatidylcholine (unpaired student t test).

As shown in Figure 13, treatment of Kv1.5 expressing *Xenopus* oocytes with lysophosphatidylcholine (1μg/ml) for 10 minutes was indeed followed by a decrease of K^+ currents.

4.3 Regulation of Kir2.1 by VP1

4.3.1 Inhibition of K^+ currents in Kir2.1 expressing *Xenopus* oocytes by coexpression of VP1 but not of [H153A]VP1

The third part of study explored, whether coexpression of parvovirus B19 capsid protein VP1 influences the activity of Kir2.1 K^+-channels. In order to test whether VP1 regulate the Kir2.1 K^+ current, Kir2.1 was expressed in *Xenopus* oocytes with or without additional expression of VP1 or the [H153A]VP1 mutant lacking functional PLA2 activity. Inwardly rectifying K^+ peak currents was taken as a measure of K^+-channel activity
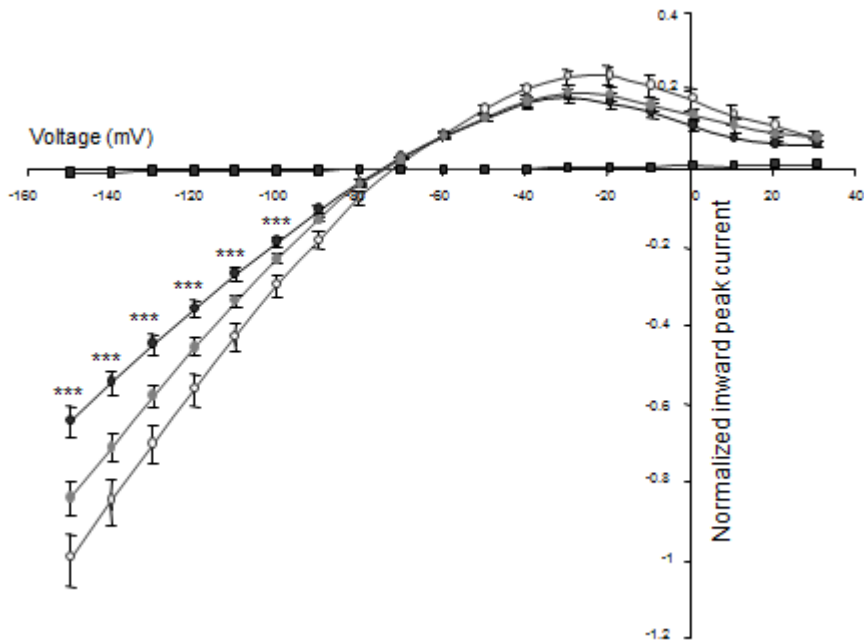
Figure 14: normalized I/V curve of KV1.5 K⁺ current with and without Coexpression of VP1 or the PLA2-negative ^{H153A}VP1 mutant

Arithmetic means ± SEM (n = 6-22) of the normalized Kir2.1 current as a function of voltage in *Xenopus* oocytes injected with water (black squares), or with cRNA encoding Kir2.1 alone (white circles) or with cRNA encoding both, Kir2.1 and VP1 (black circles) or with cRNA encoding Kir2.1 and PLA2-negative VP1 mutant (grey circles). Peak currents were normalized to the mean peak current at -150 mV in *Xenopus* oocytes injected with cRNA encoding Kir2.1. *** (p<0.001) indicates statistically significant difference from *Xenopus* oocytes injected with cRNA encoding Kir2.1 (separated unpaired student t test).

Figure 15: Effect of VP1 co-expression on K$^+$ currect in Kir2.1 expressing Xenopus oocytes

A.Original tracings recorded in *Xenopus* oocytes injected with water (i), with cRNA encoding Kir2.1 alone (ii) with cRNAs encoding both, Kir2.1 and VP1 (iii) and with cRNA encoding both, Kir2.1 and the PLA2-negative ^{H153A}VP1 mutant (iv). The currents were elicited every 20 s with 1 s pulses from -150 mV to +30 mV applied from a holding potential of -60 mV.

B.Arithmetic means ± SEM (n = 6-22) of the normalized Kir2.1 peak current at -150 mV in *Xenopus* oocytes injected with water (dotted bar), with cRNA encoding Kir2.1 alone (white bar) with cRNA encoding both, Kir2.1 and VP1 (black bar) or with cRNA encoding Kir2.1 and

<superscript>H153A</superscript>VP1 mutant (grey bar). *** (p< 0.001) indicates statistically significant difference from *Xenopus* oocytes injected with cRNA encoding Kir2.1 alone, # (p< 0.05) indicates statistically significant difference from *Xenopus* oocytes injected with cRNA encoding wild type VP1 (ANOVA-one way).

As shown in Figure 15, Inwardly rectifying currents were low in *Xenopus* oocytes injected with water. Expression of Kir2.1 resulted in a strong inwardly rectifying current (I_K). Coexpression of wild type VP1 was followed by a marked decline of I_K. In contrast coexpression of the ^{H153A}VP1 mutant lacking functional PLA2 activity, did not significantly modify Kir2.1 currents. Accordingly, the K^+ current was significantly higher following coexpression of Kir2.1 with ^{H153A}VP1 than following coexpression of Kir2.1 with VP1.

4.3.2 Inhibition of K⁺-channel activity in Kir2.1 expressing *Xenopus* oocytes by lysophosphatidylcholine

As PLA2 of VP1 is known to generate lysophosphatidylcholine, additional experiments were performed to test whether lysophosphatidylcholine influences K^+ currents in Kir2.1 expressing Xenopus oocytes. Kir2.1 expressing oocytes were treated with lysophosphatidylcholine (1µg/ml) for 10 minutes.
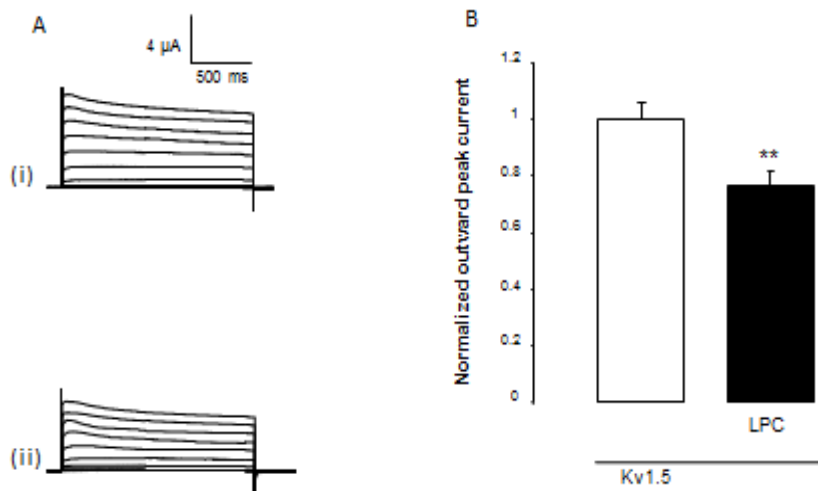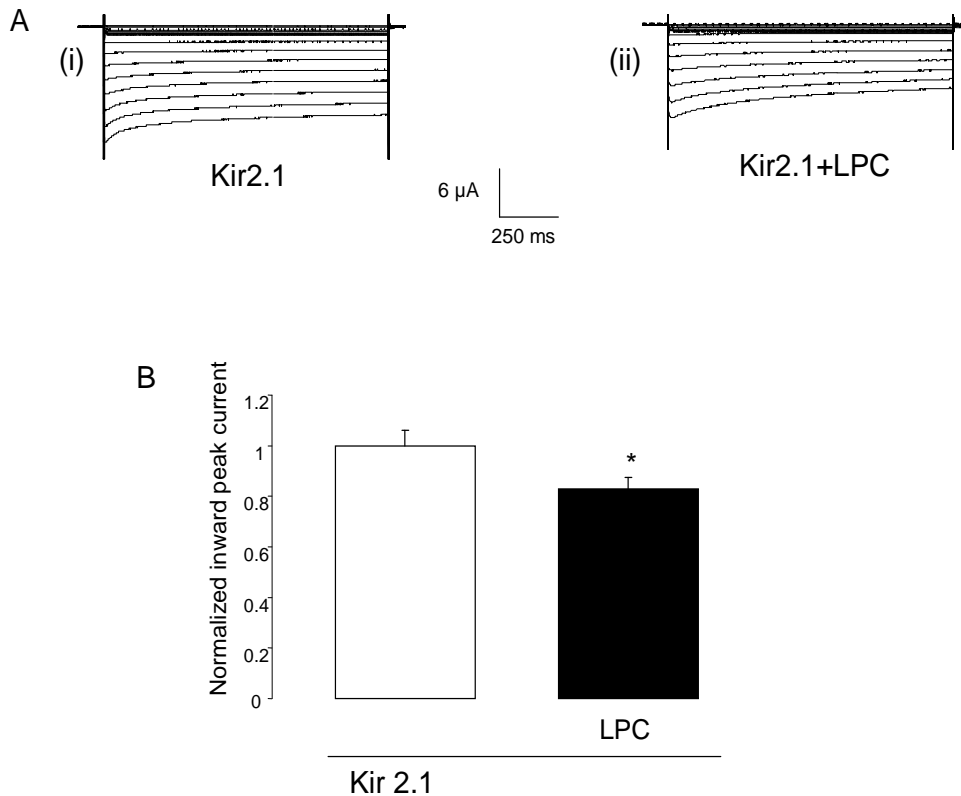
Figure 16: effect of lysophosphatidylcholine on K+ current in Kir2.1 expressing
Xenopus **oocytes**

A. Original tracings recorded in oocytes injected with cRNA encoding Kir2.1 alone in the absence (i) or presence (ii) of lysophosphatidylcholine (1 µg/ml). The currents were elicited every 20 s with 1 s pulses from -150 mV to +30 mV applied from a holding potential of -60 mV.**B.** Arithmetic means ± SEM (n = 18) of the normalized K^+-peak current in oocytes injected with cRNA encoding Kir2.1 alone in the absence (white bar) and presence (black bar) of lysophosphatidylcholine (1 µg/ml). * indicates statistically significant ($p<0.05$) difference from absence of lysophosphatidylcholine (unpaired student t test).

As shown in Figure 16, the treatment of Kir2.1 expressing *Xenopus* oocytes with lysophosphatidylcholine (1µg/ml) within 10 minutes significantly decreased the K^+ currents.

4.3.3 Inhibition of K$^+$-channel activity in Kir2.1 expressing *Xenopus* oocytes by Ouabain

Additional experiments were performed to test whether the effect of VP1 expression or lysophosphatidylcholine treatment could be mimicked by inhibition of the Na$^+$/K$^+$ ATPase with Ouabain. In order to test whether effect of VP1 expression or lysophosphatidylcholine treatment could be mimicked by inhibition of the Na$^+$/K$^+$ ATPase with ouabain, Kir2.1 expressing oocytes were treated with Ouabain (0.1 mM) for 10 minutes
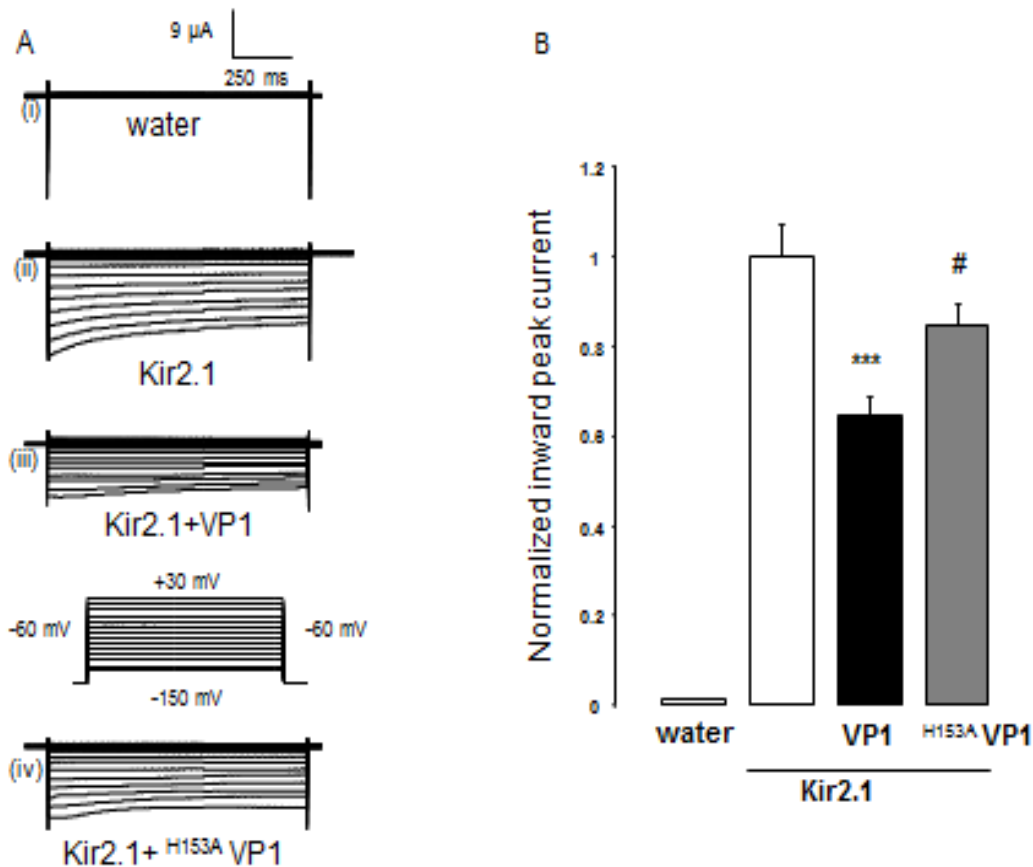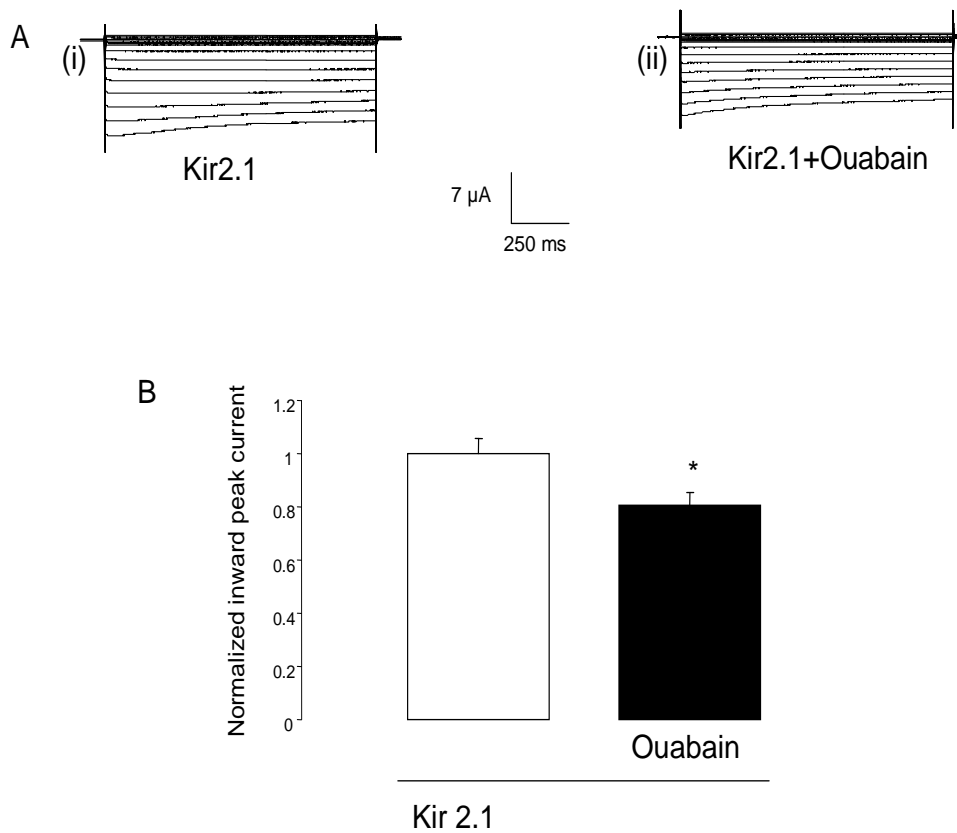
Figure 17: Effect of Ouabain on K+ current in Kir2.1 expressing Xenopus oocytes

A. Original tracings recorded in oocytes injected with cRNA encoding Kir2.1 alone in the absence (i) or presence (ii) of ouabain (0.1 mM). The currents were elicited every 20 s with 1 s pulses from -150 mV to +30 mV applied from a holding potential of -60 mV.

B. Arithmetic means ± SEM (n = 18) of the normalized K^+-peak current in oocytes injected with cRNA encoding Kir2.1 alone in the absence (white bar) and presence (black bar) of ouabain (0.1 mM). * indicates statistically significant ($p < 0.05$) difference from absence of ouabain (unpaired student t test).

As shown in Figure 17, the treatment of Kir2.1 expressing *Xenopus* oocytes with ouabain within 10 minutes significantly decreased the K^+ currents

4.3.4 Nonadditivity of lysophosphatidylcholine and ouabain on Kir2.1 K^+ channel activity

Further experiments tested, whether the inhibition of Na^+/K^+ ATPase was required for the inhibitory effect of lysophosphatidylcholine on Kir2.1. To this end, the Kir2.1 expressing *Xenopus* oocytes were treated either with lysophosphatidylcholine (1µg/ml) alone or with both lysophosphatidylcholine (1µg/ml) and ouabain (0.1 mM) for 10 minutes.
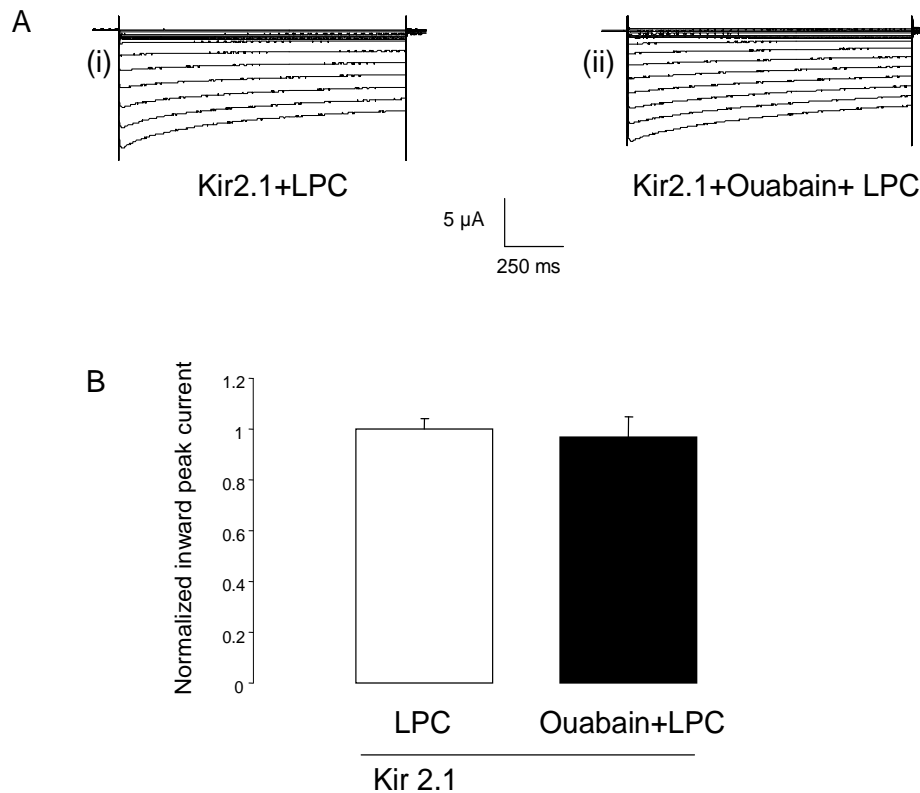
Figure 18: Nonadditivity of lysophosphatidylcholine and ouabain on Kir2.1 K$^+$ channel activity

A. Original tracings recorded in oocytes injected with cRNA encoding Kir2.1 alone and treated for 10 minutes with lysophosphatidylcholine (1 µg/ml) (i) or with both, lysophosphatidylcholine (1µg/ml) and ouabain (0.1 mM)(ii). The currents were elicited every 20 s with 1 s pulses from -150 mV to +30 mV applied from a holding potential of -60 mV.
B. Arithmetic means ± SEM (n = 19) of the normalized K$^+$-peak current in oocytes injected with cRNA encoding Kir2.1 alone in the presence of lysophosphatidylcholine (1 µg/ml) (white bar) and presence (black bar) of both lysophosphatidylcholine (1µg/ml) and ouabain (0.1 mM).

As illustrated in Figure 18, the decline of I$_K$ in Kir2.1 expressing oocytes was similar following combined treatment with lysophosphatidylcholine (1µg/ml) and ouabain (0.1 mM) and following treatment with lysophosphatidylcholine alone.

5. Discussion and Conclusion

5.1 Regulation of Kv1.3 and Kv1.5 by parvovirus B19 capsid protein VP1

Although the association between B19V infection and acute and chronic myocarditis has been revealed with the identification of myocardial endothelial cells as target cells (30, 33, 247, 275, 276) and the role of B19 as causative agent in the development of endothelial and isolated left ventricle diastolic dysfunction has been discussed (76), little is known about the pathophysiological mechanisms involved (249). Endothelial rather than myocardial B19V was detected in fatal inflammatory cardiomyopathy (33, 34).

It has been shown that parvovirus B19 capsid protein VP1 increase Ca^{2+} entry in the endothelial cells through activation of the store operated or capacitative Ca^{2+} channel (I_{CRAC}), an effect which is mimicked by the PLA2 product lysophosphatidylcholine and abolished by an inactivating mutation of the PLA2-encoding region of the VP1 protein (249). Similarly, VP1 has been shown to downregulate Na^+/K^+ ATPase, an effect is mimicked by the PLA2 product lysophosphatidylcholine and abolished by an inactivating mutation of the PLA2-encoding region of the VP1 protein (250).

The *Xenopus* oocytes expression system has played an important role in the study of cellular proteins because it is used for expression of transporters and ion channels and for functional screening for ion channels modulators (277).
Xenopus oocytes expression system was first used for expression of cellular proteins in 1971, where it was revealed that Xenopus oocytes are able to synthesize haemoglobin following intracellular injection of the corresponding mRNA (278).

In comparison to mammalian cell lines, *Xenopus* oocytes have a number of advantages as an expression system for cellular proteins. The cost of the frogs is

relatively low and frogs are easily maintained and reproduced in aquariums. Oocytes can be obtained many times from the same frog by partial ovarectomy and can survive outside the body of the frog for up to a month if conserved at 4 °C. The handling of the Xenopus oocytes is easy because they are big in size. *Xenopus* oocytes contain the necessary enzymes for the expression of a wide range of mammalian proteins (277). Following injection of cRNA into the oocyte, proteins are expressed after 1–2 days and functional studies of ion channels and receptors are easily performed using two-electrode voltage clamp technique. An important advantage is that most cRNAs are readily expressed without the need to develop a cell line, whereas there is often a delay from the cloning of a new receptor until it can be expressed in a mammalian cell line (277).

Despite the advantages of the *Xenopus* oocytes expression system, this expression system has several disadvantages. The most important of these is whether ion channels expressed in Xenopus oocytes are assembled and behave in an identical fashion to those expressed in mammalian cells. The size of the *Xenopus* oocyte is large, which gives a relatively slow fluid exchange time around the oocyte compared to a mammalian cell, which can be a problem for recording fast desensitizing ligand gated channels in the oocytes. Another disadvantage is that each oocyte must be injected with cRNAs, which is slower than the simultaneous transfection of large numbers of mammalian cells (277), However, some studies showed similar results in *Xenopus* oocytes expression system and mammalian cells (250, 279-282).

The present study was done to investigate whether parvovirus B19 capsid protein VP1 modifies the activity of Kv1.3 and Kv1.5 Potassium channels and to test whether the effect is is sensitive to inhibition of PLA2 and is mimicked by lysophosphatidylcholine using Xenopus oocytes expression system. Kv1.3 or Kv1.5 was expressed in the Xenopus oocytes with or without additional expression of VP1 and VP1 dead mutant (^{H153A}VP1) lacking functional PLA2 activity. Two

electrode voltage clamp technique was used to measure the potassium current. The measurements showed inhibition of both Kv1.3 and Kv1.5 K^+ current by VP1 but not by VP1 dead mutant (^{H153A}VP1) lacking functional PLA2 activity.

Further experiments were done to test whether the effect of VP1 on Kv1.3 and Kv1.5 potassium current is mimicked by lysophosphatidylcholine, Kv1.3 or Kv1.5 was expressed in *Xenopus* oocytes and treated by lysophosphatidylcholine (1µg/ml) for 10 minutes. Two electrode voltage clamp technique was used to measure the potassium current. The experiments showed inhibition of Kv1.3 and Kv1.5 K^+ current by lysophosphosphatidylcholine which is generated by phospholipase A2 like motif of VP1 protein.

The present observations reveal a novel action of the B19V capsid protein VP1, i.e. the downregulation of the voltage gated K^+ channels Kv1.3 and Kv1.5. The effect requires an intact phospholipase A2-like motif (283, 284) in the VP1 protein. Mutation of the motif virtually abrogates the effect of VP1 on Kv1.3 and Kv1.5. The effect of VP1 on Ca^{2+} entry (249) and Na^+/K^+ ATPase activity (250) similarly depended on phospholipase A2 activity and was similarly abolished following site directed mutation of the PLA2 motif, i.e. replacement of the histidine by alanine in the putative catalytic site (^{H153A}VP1). Similar to what has been observed previously on the regulation of Ca^{2+} entry (249) and Na^+/K^+ ATPase activity (250), the effect of VP1 expression on Kv1.3 and Kv1.5 channel activity was mimicked by lysophosphatidylcholine, a product of phospholipase A2.

B19V enters myocardial endothelial cells (33, 34) and may thus trigger acute myocarditis resulting in a clinical course similar to myocardial infarction (33, 34). Inhibition of K^+ channels could lead to cell swelling (285, 286) and could thus contribute to endothelial dysfunction. The effect is expected to be compounded by inhibition of Na^+/K^+-ATPase (250), which would dissipate the ion gradients across the cell membrane thus further compromizing the ability of the cell to maintain cell volume constancy (250). K^+ exit through K^+ channels generates a cell negative

54

potential difference across the cell membrane driving Cl$^-$ exit. Inhibition of K$^+$ channels is expected to depolarize the cell membrane thus dissipating the electrical driving force for Cl$^-$ exit. As a result, downregulation of K$^+$ channels is expected to trigger cellular accumulation of KCl with the respective osmotically obliged water and thus to swell the cells (285, 286). Cell swelling is further fostered by cellular NaCl accumulation, if Na$^+$/K$^+$ATPase activity is inhibited (250).

Inhibition of Kv1.3 K$^+$ channels may further affect cell proliferation, which, at least in some cell types, requires Kv1.3 channel activity (252, 253). Whether or not impaired endothelial cell proliferation may contribute to the pathophysiology of B19V infection remains to be shown.

In conclusion, VP1 down-regulates the Kv1.3 and Kv1.5 K$^+$ channel, an effect involving phospholipase A2 activity of the parvoviral B19 protein and genetration of lysophosphatidylcholine. The inhibition of endothelial K$^+$ channels may lead to cell swelling and thus participate in the pathophysiology of endothelial dysfunction during parvovirus B19 infection.
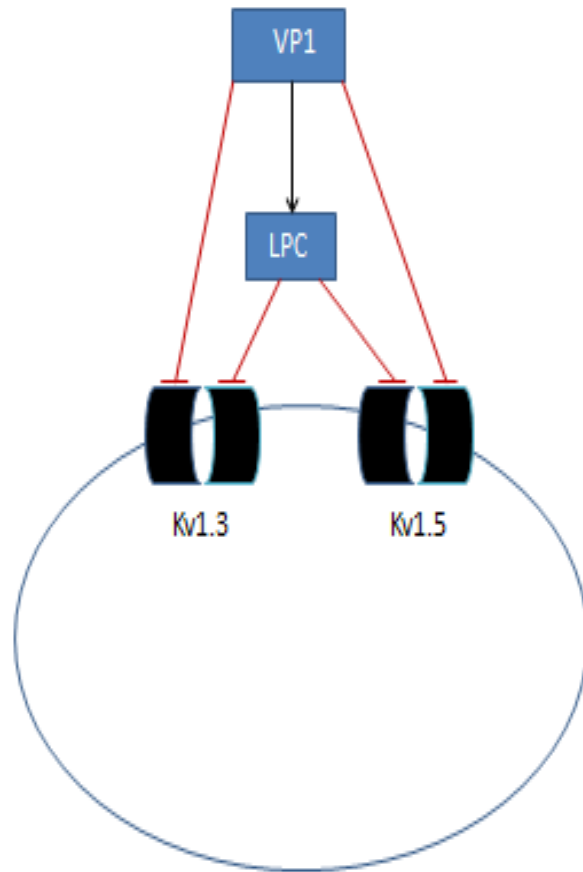
Figure 19: Summary of regulation of Kv1.3 and Kv1.5 by VP1

5.2 Regulation of Kir2.1 by parvovirus B19 capsid protein VP1

B19V is a worldwide infectious pathogen in humans as the estimated prevalence of IgG antibodies directed against B19V ranges from 2 to 15% in children at age of 1 to 5 years old, 15 to 60% in children aged 6 to 19 years old, 30 to 60% in adults, and more than 85% in the geriatric population(35-38).

B19V causes common infections (245) leading to diverse clinical entities, such as fifth disease (erythema infectiosum), hydrops fetalis and transient aplastic anaemia (25, 287). More importantly B19V infection is associated with myocarditis (246, 247).

It is known that the myocardial endothelium is as a target for parvovirus B19 in acute and chronic myocarditis (30, 33, 247, 275, 276) And it has been shown that B19V is a causative agent in endothelial and left ventricle diastolic dysfunction (76), but the pathophysiological mechanisms involved are still not known(249). Parvovirus B19 genomes were detected in the endothelium of myocardial tissue predominantly of small intramyocardial arteries and venoles, but not in cardiac myocytes or epicardial coronaries in fatal inflammatory cardiomyopathy. The presence of B19V genomes is accompanied with expression of the adhesion molecule E-selectin, margination, adherence, penetration, and perivascular infiltration of the heart by T-lymphocytes and macrophages function (33, 34)

It has been shown that parvovirus B19 capsid protein VP1 increase Ca^{2+} entry in the endothelial cells through activation of the store operated or capacitative Ca^{2+} channel (I_{CRAC}), an effect which was mimicked by the PLA2 product lysophosphatidylcholine and abolished by an inactivating mutation of the PLA2-encoding region of the VP1 protein (249). Similarly, VP1 has been shown to downregulate Na^+/K^+ ATPase, an effect was mimicked by the PLA2 product

lysophosphatidylcholine and abolished by an inactivating mutation of the PLA2-encoding region of the VP1 protein (250).

This study was done to investigate whether parvovirus B19 capsid protein VP1 modifies the activity of inwardly rectifying Kir2.1 Potassium channels and to test whether the effect is is sensitive to inhibition of PLA2 and is mimicked by lysophosphatidylcholine using *Xenopus* oocytes expression system. Kir2.1 was expressed in the *Xenopus* oocytes with or without additional expression of VP1 and VP1 dead mutant (^{H153A}VP1) lacking functional PLA2 activity. Two electrode voltage clamp technique was used to measure the potassium current. The experiments have shown inhibition of Kir2.1 K$^+$ current by VP1 but not by VP1 dead mutant (^{H153A}VP1) lacking functional PLA2 activity.

Another set of experiments were done to test whether the effect of VP1 on Kir2.1 K+ current is mimicked by lysophosphatidylcholine, Kir2.1 was expressed in Xenopus oocytes and was treated by lysophosphatidylcholine (1µg/ml) for 10 minutes. Two electrode voltage clamp technique was used to measure the potassium current. These experiments have shown inhibition of Kir2.1 Potassium current by Lysophosphosphatidylcholine which is generated by phospholipase A2 like motif of VP1 protein.

The present observations disclose a novel effect of the B19V capsid protein VP1, i.e. the downregulation of the inwardly rectifying K$^+$ channel Kir2.1. As shown previously for Kv1.3 and Kv1.5 channels (288), Ca^{2+} entry(249) and Na$^+$/K$^+$ ATPase activity (250), the effect of VP1 requires its phospholipase A2-like motif (21, 24). Loss of function mutation of the motif disrupts the effect of VP1 on Kir2.1. Again, similar to what has been observed previously on the regulation of voltage gated K$^+$ channels (288), Ca^{2+} entry (249) and Na$^+$/K$^+$ ATPase activity (250), the effect of VP1 expression on Kir2.1 channel activity was mimicked by the vPLA2 product lysophosphatidylcholine.

The effect of B19V on K^+ channels could contribute to the triggering of endothelial dysfunction, as B19V enters myocardial endothelial cells (33, 34). Inhibition of K^+ channels is expected to foster cell swelling (285, 286), as reduced K^+ channel activity leads to impaired K^+ exit, depolarization, Cl^- entry and thus cellular accumulation of KCl with the respective osmotically obliged water swelling (285, 286). The depolarization is further fostered by inhibition of Na^+/K^+-ATPase activity (250) with the resulting dissipation of the ion gradients across the cell membrane.

The inhibition of Kir2.1 channels could at least partially result from the inhibitory effect of lysophosphatidylcholine on the Na^+/K^+-ATPase (250), as the channels are similarly downregulated by the Na^+/K^+-ATPase inhibitor ouabain. Inwardly rectifying K^+ channels have previously been shown to be highly sensitive to Na^+/K^+-ATPase activity and to be rapidly down regulated following pump inhibition (239).

Since functional expression of classical Kir channels provides the driving force for Ca^{2+} influx through Ca^{2+}-permeable channels by seting the E_{res} of endothelial cells to a negative potential, inhibition of endothelial Kir channels is expected to inhibit both flow induced Ca^{2+} influx and vasodilatation caused by Ca^{2+} dependent production of Nitric Oxide (224, 225).

In conclusion, VP1 down-regulates the inwardly rectifying K^+ channel Kir2.1, an effect involving phospholipase A2 activity of the parvoviral B19 protein, lysophosphatidylcholine formation, and inhibition of Na^+/K^+-ATPase activity. The inhibition of endothelial K^+ channels may lead to cell swelling and thus participate in the pathophysiology of endothelial dysfunction during parvovirus B19 infection.
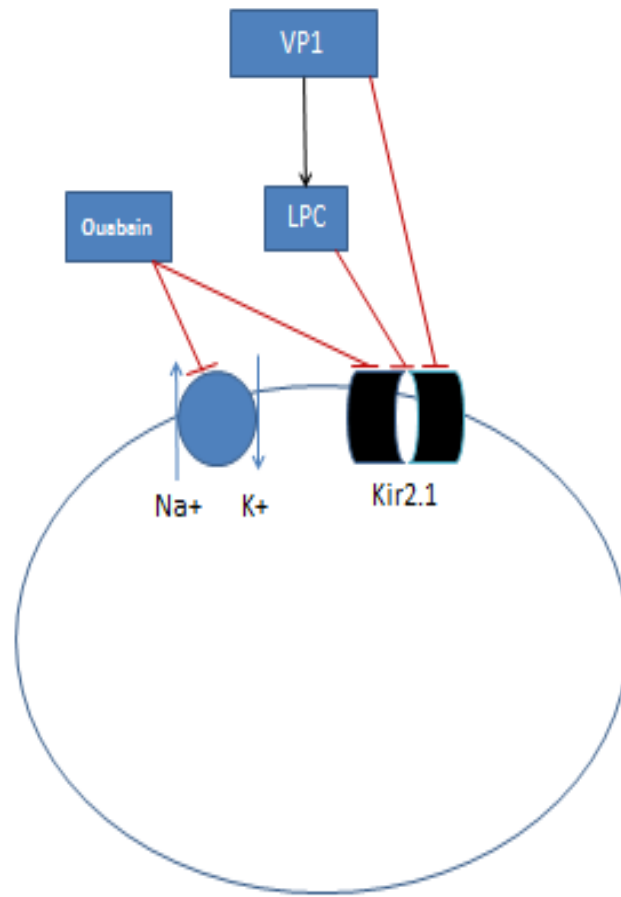
Figure 20: Summary of regulation of Kir2.1 by VP1

6. Summary

Parvovirus B19 (B19V) can cause inflammatory cardiomyopathy and endothelial dysfunction. Pathophysiological mechanisms involved include lysophosphatidylcholine producing phospholipase A2 (PLA2) activity of the B19V capsid protein VP1. Most recently, VP1 and lysophosphatidylcholine have been shown to inhibit Na^+/K^+ ATPase. The present study explored whether VP1 modifies the activity of Kv1.3, Kv1.5 and Kir2.1 K^+ channels.

The first part of study explored, whether expression of VP1 modifies the activity of Kv1.3 and Kv1.5 K^+ channels. cRNA encoding Kv1.3 or Kv1.5 was injected into *Xenopus* oocytes without or with cRNA encoding VP1,which was isolated from a patient suffering from fatal B19V induced myocarditis or the VP1 mutant $^{H153A}VP1$ lacking a functional PLA2 activity. K^+ channel activity was determined by dual electrode voltage clamp. Injection of cRNA encoding Kv1.3 or Kv1.5 into *Xenopus* oocytes was followed by appearance of Kv K^+ channel activity, which was significantly decreased by additional injection of cRNA encoding VP1, but not by additional injection of cRNA encoding PLA2-negative VP1 mutant $^{H153A}VP1$. The effect of VP1 on Kv current was not significantly modified by transcription inhibitor actinomycin (10 µM for 36 hours) but was mimicked by lysophosphatidylcholine (1 µg/ml).

The B19V capsid protein VP1 inhibits host cell Kv channels, an effect at least partially due to phospholipase A2 (PLA2) dependent formation of lysophosphatidylcholine.

The second part of study explored, whether expression of VP1 influences the activity of the inwardly rectifying Kir2.1 K^+ channels. cRNA encoding Kir2.1 was injected into *Xenopus* oocytes without or with cRNA encoding VP1 or the VP1 mutant $^{H153A}VP1$. K^+ channel activity was determined by dual electrode voltage clamp. Injection of cRNA encoding Kir2.1 into *Xenopus* oocytes was followed by appearance of inwardly rectifying K^+ channel activity (I_K), which was significantly decreased by additional injection of cRNA encoding VP1, but not by additional

injection of cRNA encoding ^{H153A}VP1. The effect of VP1 on I_K was mimicked by lysophosphatidylcholine (1 µg/ml) and by inhibition of Na$^+$/K$^+$-ATPase with 0.1 mM ouabain. In the presence of lysophosphatidylcholine, I_K was not further decreased by additional treatment with ouabain.

The B19V capsid protein VP1 inhibits Kir2.1 channels, an effect at least partially due to phospholipase A2 (PLA2) dependent formation of lysophosphatidylcholine with subsequent inhibition of Na$^+$/K$^+$-ATPase activity.

7. Zusammenfassung

Der Parvovirus B19 (B19V) kann entzündliche Kardiomyopathie und endotheliale Dysfunktion verursachen. Die beteiligten pathophysiologischen Mechanismen beinhalten die Lysophosphatidylcholin produzierende Phospholipase A2 (PLA2) Aktivität des B19V Capsidprotein VP1. So ist bereits gezeigt worden, dass VP1 und Lysophosphatidylcholin die Na^+ / K^+ -ATPase hemmen. In der vorliegenden Arbeit wurde untersucht, ob VP1 die Aktivität der Kv1.3, Kv1.5 und Kir2.1 K^+ Kanäle ändert.

Im ersten Teil der Arbeit wurde untersucht, ob die Expression des VP1 die Aktivität von Kv1.3 und Kv1.5 K^+ Kanäle verändert. Die cRNA des Kv1.3 oder Kv1.5 wurde in Xenopus-Oozyten sowohl mit als auch ohne cRNA des VP1 injiziert, welches von einem an B19V verstorbenen Myokarditispatienten stammte, und einer VP1-Mutante ^{H153A}VP1 mit fehlenden funktionellen PLA2-Aktivität. Die K + -Kanal-Aktivität wurde mittels der 2-Elektroden-Voltage-Clamp-Methode ermittelt. Die Injektion der Kv1.3 oder Kv1.5 cRNA in Xenopus Oozyten führte zum Auftreten der Aktivität des Kv-K^+ -Kanals, durch zusätzliche Injektion der VP1-cRNA signifikant welche verringert wurde. Dies konnte nicht nach der Injektion der PLA2-negative Mutante VP1 ^{H153A}VP1 beobachtet werden. Der Effekt von VP1 auf den Kv Strom wurde nicht signifikant durch den Transkriptionsinhibitor Actinomycin (36 Stunden 10 & mgr; M) modifiziert und war ähnlich wie nach der Zugabe von Lysophosphatidylcholin (1 ug / ml)

Das B19V Capsidprotein VP1 hemmt in der Wirtszelle die Kv-Kanäle, welche teilweise einen Effekt der Phospholipase A2 (PLA2) abhängigen Bildung auf Lysophosphatidylcholin hat.

Im zweiten Teil der Arbeit wurde untersucht, ob die Expression des VP1 die Aktivität der einwärtsgerichteten Kir2.1 K + -Kanälen beeinflusst. Die Kir2.1 cRNA wurde sowohl mit als auch ohne VP1-cRNA oder mit der VP1-Mutante ^{H153A}VP1 in Xenopus-Oozyten injiziert. Die K^+ -Kanal-Aktivität wurde mit der 2-Elektroden-Voltage-Clamp-Methode ermittelt. Die Injektion der Kir2.1-cRNA in Xenopus-

Oozyten führte zum Auftreten einer nach innen gleichgerichtenten K + -Kanal-Aktivität (IK), die durch zusätzliche Injektion von codierter VP1-cRNA signifikant verringert war, jedoch nicht durch zusätzliche Injektion von H153AVP1-cRNA. Der Effekt von VP1 auf die IK war ähnlich wie nach der Zugabe von Lysophosphatidylcholin (1 ug / ml) und Hemmung der Na^+/K^+-ATPase mit 0,1 mM Ouabain. Der Ik Strom wurde unter Lysophosphatidylcholin nicht weiter durch Zugabe von Ouabain verringert.

Das B19V Capsidprotein VP1 hemmt Kir2.1-Kanäle, ein Effekt der zumindest teilweise auf der Phospholipase A2 (PLA2) abhängigen Bildung von Lysophosphatidylcholin mit anschließender Hemmung der Na^+ / K^+ -ATPase-Aktivität zurückzuführen ist.

References

1.   Cossart YE, Field AM, Cant B, Widdows D. Parvovirus-like particles in human sera. Lancet. 1975;1(7898):72-3.
2.   Heegaard ED, Brown KE. Human parvovirus B19. Clinical microbiology reviews. 2002;15(3):485-505.
3.   Deiss V, Tratschin JD, Weitz M, Siegl G. Cloning of the human parvovirus B19 genome and structural analysis of its palindromic termini. Virology. 1990;175(1):247-54.
4.   Luo W, Astell CR. A novel protein encoded by small RNAs of parvovirus B19. Virology. 1993;195(2):448-55.
5.   Ozawa K, Ayub J, Hao YS, Kurtzman G, Shimada T, Young N. Novel transcription map for the B19 (human) pathogenic parvovirus. Journal of virology. 1987;61(8):2395-406.
6.   Cotmore SF, McKie VC, Anderson LJ, Astell CR, Tattersall P. Identification of the major structural and nonstructural proteins encoded by human parvovirus B19 and mapping of their genes by procaryotic expression of isolated genomic fragments. Journal of virology. 1986;60(2):548-57.
7.   Ozawa K, Young N. Characterization of capsid and noncapsid proteins of B19 parvovirus propagated in human erythroid bone marrow cell cultures. Journal of virology. 1987;61(8):2627-30.
8.   Shade RO, Blundell MC, Cotmore SF, Tattersall P, Astell CR. Nucleotide sequence and genome organization of human parvovirus B19 isolated from the serum of a child during aplastic crisis. Journal of virology. 1986;58(3):921-36.
9.   Christensen J, Cotmore SF, Tattersall P. Minute virus of mice transcriptional activator protein NS1 binds directly to the transactivation region of the viral P38 promoter in a strictly ATP-dependent manner. Journal of virology. 1995;69(9):5422-30.
10.   Christensen J, Cotmore SF, Tattersall P. A novel cellular site-specific DNA-binding protein cooperates with the viral NS1 polypeptide to initiate parvovirus DNA replication. Journal of virology. 1997;71(2):1405-16.
11.   Cotmore SF, Christensen J, Nuesch JP, Tattersall P. The NS1 polypeptide of the murine parvovirus minute virus of mice binds to DNA sequences containing the motif [ACCA]2-3. Journal of virology. 1995;69(3):1652-60.
12.   Doerig C, Hirt B, Antonietti JP, Beard P. Nonstructural protein of parvoviruses B19 and minute virus of mice controls transcription. Journal of virology. 1990;64(1):387-96.
13.   Wilson GM, Jindal HK, Yeung DE, Chen W, Astell CR. Expression of minute virus of mice major nonstructural protein in insect cells: purification and identification of ATPase and helicase activities. Virology. 1991;185(1):90-8.

14.   Mitchell LA. Parvovirus B19 nonstructural (NS1) protein as a transactivator of interleukin-6 synthesis: common pathway in inflammatory sequelae of human parvovirus infections? J Med Virol. 2002;67(2):267-74.

15.   Hsu TC, Wu WJ, Chen MC, Tsay GJ. Human parvovirus B19 non-structural protein (NS1) induces apoptosis through mitochondria cell death pathway in COS-7 cells. Scand J Infect Dis. 2004;36(8):570-7.

16.   Moffatt S, Yaegashi N, Tada K, Tanaka N, Sugamura K. Human parvovirus B19 nonstructural (NS1) protein induces apoptosis in erythroid lineage cells. Journal of virology. 1998;72(4):3018-28.

17.   Sol N, Le Junter J, Vassias I, Freyssinier JM, Thomas A, Prigent AF, et al. Possible interactions between the NS-1 protein and tumor necrosis factor alpha pathways in erythroid cell apoptosis induced by human parvovirus B19. Journal of virology. 1999;73(10):8762-70.

18.   Duechting A, Tschope C, Kaiser H, Lamkemeyer T, Tanaka N, Aberle S, et al. Human parvovirus B19 NS1 protein modulates inflammatory signaling by activation of STAT3/PIAS3 in human endothelial cells. Journal of virology. 2008;82(16):7942-52.

19.   Gigler A, Dorsch S, Hemauer A, Williams C, Kim S, Young NS, et al. Generation of neutralizing human monoclonal antibodies against parvovirus B19 proteins. Journal of virology. 1999;73(3):1974-9.

20.   Young NS, Brown KE. Parvovirus B19. N Engl J Med. 2004;350(6):586-97.

21.   Canaan S, Zadori Z, Ghomashchi F, Bollinger J, Sadilek M, Moreau ME, et al. Interfacial enzymology of parvovirus phospholipases A2. J Biol Chem. 2004;279(15):14502-8.

22.   Li Y, Zadori Z, Bando H, Dubuc R, Fediere G, Szelei J, et al. Genome organization of the densovirus from Bombyx mori (BmDNV-1) and enzyme activity of its capsid. The Journal of general virology. 2001;82(Pt 11):2821-5.

23.   Zadori Z, Szelei J, Lacoste MC, Li Y, Gariepy S, Raymond P, et al. A viral phospholipase A2 is required for parvovirus infectivity. Dev Cell. 2001;1(2):291-302.

24.   Dorsch S, Liebisch G, Kaufmann B, von Landenberg P, Hoffmann JH, Drobnik W, et al. The VP1 unique region of parvovirus B19 and its constituent phospholipase A2-like activity. Journal of virology. 2002;76(4):2014-8.

25.   Young NS, Brown KE. Parvovirus B19. N Engl J Med. 2004;350(6):586-97.

26.   Brown KE, Anderson SM, Young NS. Erythrocyte P antigen: cellular receptor for B19 parvovirus. Science. 1993;262(5130):114-7.

27.   Brown KE, Cohen BJ. Haemagglutination by parvovirus B19. The Journal of general virology. 1992;73 (Pt 8):2147-9.

28.   Brown KE, Hibbs JR, Gallinella G, Anderson SM, Lehman ED, McCarthy P, et al. Resistance to parvovirus B19 infection due to lack of virus receptor (erythrocyte P antigen). N Engl J Med. 1994;330(17):1192-6.

29.   Brown KE, Anderson SM, Young NS. Erythrocyte P antigen: cellular receptor for B19 parvovirus. Science. 1993;262(5130):114-7.

30.   Weigel-Kelley KA, Yoder MC, Srivastava A. Alpha5beta1 integrin as a cellular coreceptor for human parvovirus B19: requirement of functional activation of beta1 integrin for viral entry. Blood. 2003;102(12):3927-33.

31.   Munakata Y, Saito-Ito T, Kumura-Ishii K, Huang J, Kodera T, Ishii T, et al. Ku80 autoantigen as a cellular coreceptor for human parvovirus B19 infection. Blood. 2005.

32.   Ellis PD, Metcalfe JC, Hyvonen M, Kemp PR. Adhesion of endothelial cells to NOV is mediated by the integrins alphavbeta3 and alpha5beta1. J Vasc Res. 2003;40(3):234-43.

33.   Bultmann BD, Klingel K, Sotlar K, Bock CT, Baba HA, Sauter M, et al. Fatal parvovirus B19-associated myocarditis clinically mimicking ischemic heart disease: an endothelial cell-mediated disease. Hum Pathol. 2003;34(1):92-5.

34.   Klingel K, Sauter M, Bock CT, Szalay G, Schnorr JJ, Kandolf R. Molecular pathology of inflammatory cardiomyopathy. Med Microbiol Immunol (Berl). 2004;193(2-3):101-7.

35.   Anderson LJ, Tsou C, Parker RA, Chorba TL, Wulff H, Tattersall P, et al. Detection of antibodies and antigens of human parvovirus B19 by enzyme-linked immunosorbent assay. Journal of clinical microbiology. 1986;24(4):522-6.

36.   Cohen BJ, Buckley MM. The prevalence of antibody to human parvovirus B19 in England and Wales. Journal of medical microbiology. 1988;25(2):151-3.

37.   Kelly HA, Siebert D, Hammond R, Leydon J, Kiely P, Maskill W. The age-specific prevalence of human parvovirus immunity in Victoria, Australia compared with other parts of the world. Epidemiology and infection. 2000;124(3):449-57.

38.   Tsujimura M, Matsushita K, Shiraki H, Sato H, Okochi K, Maeda Y. Human parvovirus B19 infection in blood donors. Vox sanguinis. 1995;69(3):206-12.

39.   Koch WC, Adler SP. Human parvovirus B19 infections in women of childbearing age and within families. The Pediatric infectious disease journal. 1989;8(2):83-7.

40.   Prospective study of human parvovirus (B19) infection in pregnancy. Public Health Laboratory Service Working Party on Fifth Disease. Bmj. 1990;300(6733):1166-70.

41.   Evans JP, Rossiter MA, Kumaran TO, Marsh GW, Mortimer PP. Human parvovirus aplasia: case due to cross infection in a ward. British medical journal. 1984;288(6418):681.

42.   Cohen BJ, Courouce AM, Schwarz TF, Okochi K, Kurtzman GJ. Laboratory infection with parvovirus B19. Journal of clinical pathology. 1988;41(9):1027-8.

43.   Woolf AD, Campion GV, Chishick A, Wise S, Cohen BJ, Klouda PT, et al. Clinical manifestations of human parvovirus B19 in adults. Archives of internal medicine. 1989;149(5):1153-6.

44.   Cartter ML, Farley TA, Rosengren S, Quinn DL, Gillespie SM, Gary GW, et al. Occupational risk factors for infection with parvovirus B19 among pregnant women. The Journal of infectious diseases. 1991;163(2):282-5.

45.   Anderson MJ, Davis LR, Hodgson J, Jones SE, Murtaza L, Pattison JR, et al. Occurrence of infection with a parvovirus-like agent in children with sickle cell anaemia during a two-year period. Journal of clinical pathology. 1982;35(7):744-9.

46.   Anderson MJ, Higgins PG, Davis LR, Willman JS, Jones SE, Kidd IM, et al. Experimental parvoviral infection in humans. The Journal of infectious diseases. 1985;152(2):257-65.

47.   Naides SJ. Infection with Parvovirus B19. Current infectious disease reports. 1999;1(3):273-8.

48.   Zerbini M, Musiani M, Venturoli S, Gallinella G, Gibellini D, Gentilomi G, et al. Different syndromes associated with B19 parvovirus viraemia in paediatric patients: report of four cases. European journal of pediatrics. 1992;151(11):815-7.

49.   Reid DM, Reid TM, Brown T, Rennie JA, Eastmond CJ. Human parvovirus-associated arthritis: a clinical and laboratory description. Lancet. 1985;1(8426):422-5.

50.   White DG, Woolf AD, Mortimer PP, Cohen BJ, Blake DR, Bacon PA. Human parvovirus arthropathy. Lancet. 1985;1(8426):419-21.

51.   Nocton JJ, Miller LC, Tucker LB, Schaller JG. Human parvovirus B19-associated arthritis in children. The Journal of pediatrics. 1993;122(2):186-90.

52.   Joseph PR. Fifth disease: the frequency of joint involvement in adults. New York state journal of medicine. 1986;86(11):560-3.

53.   Woolf AD. Human parvovirus B19 and arthritis. Behring Institute Mitteilungen. 1990(85):64-8.

54.   Naides SJ. Rheumatic manifestations of parvovirus B19 infection. Rheumatic diseases clinics of North America. 1998;24(2):375-401.

55.   Naides SJ, Scharosch LL, Foto F, Howard EJ. Rheumatologic manifestations of human parvovirus B19 infection in adults. Initial two-year clinical experience. Arthritis and rheumatism. 1990;33(9):1297-309.

56.   Brown T, Anand A, Ritchie LD, Clewley JP, Reid TM. Intrauterine parvovirus infection associated with hydrops fetalis. Lancet. 1984;2(8410):1033-4.

57.   Katz VL, McCoy MC, Kuller JA, Hansen WF. An association between fetal parvovirus B19 infection and fetal anomalies: a report of two cases. American journal of perinatology. 1996;13(1):43-5.

58.   Tiessen RG, van Elsacker-Niele AM, Vermeij-Keers C, Oepkes D, van Roosmalen J, Gorsira MC. A fetus with a parvovirus B19 infection and congenital anomalies. Prenatal diagnosis. 1994;14(3):173-6.

59.   Anand A, Gray ES, Brown T, Clewley JP, Cohen BJ. Human parvovirus infection in pregnancy and hydrops fetalis. N Engl J Med. 1987;316(4):183-6.

60.   Caul EO, Usher MJ, Burton PA. Intrauterine infection with human parvovirus B19: a light and electron microscopy study. J Med Virol. 1988;24(1):55-66.

61.   Wright C, Hinchliffe SA, Taylor C. Fetal pathology in intrauterine death due to parvovirus B19 infection. Br J Obstet Gynaecol. 1996;103(2):133-6.

62.   Morey AL, Keeling JW, Porter HJ, Fleming KA. Clinical and histopathological features of parvovirus B19 infection in the human fetus. Br J Obstet Gynaecol. 1992;99(7):566-74.

63.   Bruu AL, Flugsrud LB. [Erythema infectiosum in pregnancy. A follow-up of children after 2 years]. Tidsskrift for den Norske laegeforening : tidsskrift for praktisk medicin, ny raekke. 1994;114(3):308-10.

64.   Harger JH, Adler SP, Koch WC, Harger GF. Prospective evaluation of 618 pregnant women exposed to parvovirus B19: risks and symptoms. Obstetrics and gynecology. 1998;91(3):413-20.

65.   Kerr JR, O'Neill HJ, Coyle PV, Thompson W. An outbreak of parvovirus B19 infection; a study of clinical manifestations and the incidence of fetal loss. Irish journal of medical science. 1994;163(2):65-7.

66.   Anderson LJ. Role of parvovirus B19 in human disease. The Pediatric infectious disease journal. 1987;6(8):711-8.

67.   Enders G, Biber M. Parvovirus B19 infections in pregnancy. Behring Institute Mitteilungen. 1990(85):74-8.

68.   Essary LR, Vnencak-Jones CL, Manning SS, Olson SJ, Johnson JE. Frequency of parvovirus B19 infection in nonimmune hydrops fetalis and utility of three diagnostic methods. Hum Pathol. 1998;29(7):696-701.

69.   Forestier F, Tissot JD, Vial Y, Daffos F, Hohlfeld P. Haematological parameters of parvovirus B19 infection in 13 fetuses with hydrops foetalis. British journal of haematology. 1999;104(4):925-7.

70.   Guidozzi F, Ballot D, Rothberg AD. Human B19 parvovirus infection in an obstetric population. A prospective study determining fetal outcome. The Journal of reproductive medicine. 1994;39(1):36-8.

71.	Rodis JF, Borgida AF, Wilson M, Egan JF, Leo MV, Odibo AO, et al. Management of parvovirus infection in pregnancy and outcomes of hydrops: a survey of members of the Society of Perinatal Obstetricians. American journal of obstetrics and gynecology. 1998;179(4):985-8.

72.	Schwarz TF, Nerlich A, Roggendorf M. Parvovirus B19 infection in pregnancy. Behring Institute Mitteilungen. 1990(85):69-73.

73.	Yaegashi N, Niinuma T, Chisaka H, Uehara S, Okamura K, Shinkawa O, et al. Serologic study of human parvovirus B19 infection in pregnancy in Japan. The Journal of infection. 1999;38(1):30-5.

74.	Yaegashi N, Niinuma T, Chisaka H, Watanabe T, Uehara S, Okamura K, et al. The incidence of, and factors leading to, parvovirus B19-related hydrops fetalis following maternal infection; report of 10 cases and meta-analysis. The Journal of infection. 1998;37(1):28-35.

75.	Schild RL, Bald R, Plath H, Eis-Hubinger AM, Enders G, Hansmann M. Intrauterine management of fetal parvovirus B19 infection. Ultrasound in obstetrics & gynecology : the official journal of the International Society of Ultrasound in Obstetrics and Gynecology. 1999;13(3):161-6.

76.	Tschope C, Bock CT, Kasner M, Noutsias M, Westermann D, Schwimmbeck PL, et al. High prevalence of cardiac parvovirus B19 infection in patients with isolated left ventricular diastolic dysfunction. Circulation. 2005;111(7):879-86.

77.	Bock CT, Klingel K, Kandolf R. Human parvovirus B19-associated myocarditis. N Engl J Med. 2010;362(13):1248-9.

78.	Brown KE. What threat is human parvovirus B19 to the fetus? A review. Br J Obstet Gynaecol. 1989;96(7):764-7.

79.	Crane J. Parvovirus B19 infection in pregnancy. J Obstet Gynaecol Can. 2002;24(9):727-43.

80.	Katz VL, Chescheir NC, Bethea M. Hydrops fetalis from B19 parvovirus infection. J Perinatol. 1990;10(4):366-8.

81.	Oyer CE, Ongcapin EH, Ni J, Bowles NE, Towbin JA. Fatal intrauterine adenoviral endomyocarditis with aortic and pulmonary valve stenosis: diagnosis by polymerase chain reaction. Hum Pathol. 2000;31(11):1433-5.

82.	Telerman A, Tuynder M, Dupressoir T, Robaye B, Sigaux F, Shaulian E, et al. A model for tumor suppression using H-1 parvovirus. Proc Natl Acad Sci USA. 1993;90(18):8702-6.

83.	Janner D, Bork J, Baum M, Chinnock R. Severe pneumonia after heart transplantation as a result of human parvovirus B19. The Journal of heart and lung transplantation : the official publication of the International Society for Heart Transplantation. 1994;13(2):336-8.

84.	Nour B, Green M, Michaels M, Reyes J, Tzakis A, Gartner JC, et al. Parvovirus B19 infection in pediatric transplant patients. Transplantation. 1993;56(4):835-8.

85.	Schowengerdt KO, Ni J, Denfield SW, Gajarski RJ, Bowles NE, Rosenthal G, et al. Association of parvovirus B19 genome in children with myocarditis and cardiac allograft rejection: diagnosis using the polymerase chain reaction. Circulation. 1997;96(10):3549-54.

86.	Schowengerdt KO, Ni J, Denfield SW, Gajarski RJ, Radovancevic B, Frazier HO, et al. Diagnosis, surveillance, and epidemiologic evaluation of viral infections in pediatric cardiac transplant recipients with the use of the polymerase chain reaction. The Journal of heart and lung transplantation : the official publication of the International Society for Heart Transplantation. 1996;15(2):111-23.

87.	Balfour HH, Jr., Schiff GM, Bloom JE. Encephalitis associated with erythema infectiosum. The Journal of pediatrics. 1970;77(1):133-6.

88.	Breese C, Horner FA. Encephalopathy with erythema infectiosum. American journal of diseases of children. 1977;131(1):65-7.

89.   Heegaard ED, Peterslund NA, Hornsleth A. Parvovirus B19 infection associated with encephalitis in a patient suffering from malignant lymphoma. Scand J Infect Dis. 1995;27(6):631-3.
90.   Cassinotti P, Schultze D, Schlageter P, Chevili S, Siegl G. Persistent human parvovirus B19 infection following an acute infection with meningitis in an immunocompetent patient. European journal of clinical microbiology & infectious diseases : official publication of the European Society of Clinical Microbiology. 1993;12(9):701-4.
91.   van de Vusse AC, Goossens VJ, Kemler MA, Weber WE. Screening of patients with complex regional pain syndrome for antecedent infections. The Clinical journal of pain. 2001;17(2):110-4.
92.   Denning DW, Amos A, Rudge P, Cohen BJ. Neuralgic amyotrophy due to parvovirus infection. Journal of neurology, neurosurgery, and psychiatry. 1987;50(5):641-2.
93.   Yoto Y, Kudoh T, Haseyama K, Suzuki N, Chiba S. Human parvovirus B19 infection associated with acute hepatitis. Lancet. 1996;347(9005):868-9.
94.   Yoto Y, Kudoh T, Asanuma H, Numazaki K, Tsutsumi Y, Nakata S, et al. Transient disturbance of consciousness and hepatic dysfunction associated with human parvovirus B19 infection. Lancet. 1994;344(8922):624-5.
95.   Langnas AN, Markin RS, Cattral MS, Naides SJ. Parvovirus B19 as a possible causative agent of fulminant liver failure and associated aplastic anemia. Hepatology. 1995;22(6):1661-5.
96.   Tsuda H. Liver dysfunction caused by parvovirus B19. The American journal of gastroenterology. 1993;88(9):1463.
97.   West NC, Meigh RE, Mackie M, Anderson MJ. Parvovirus infection associated with aplastic crisis in a patient with HEMPAS. Journal of clinical pathology. 1986;39(9):1019-20.
98.   Chorba T, Coccia P, Holman RC, Tattersall P, Anderson LJ, Sudman J, et al. The role of parvovirus B19 in aplastic crisis and erythema infectiosum (fifth disease). The Journal of infectious diseases. 1986;154(3):383-93.
99.   Doran HM, Teall AJ. Neutropenia accompanying erythroid aplasia in human parvovirus infection. British journal of haematology. 1988;69(2):287-8.
100.   Lefrere JJ, Courouce AM, Bertrand Y, Girot R, Soulier JP. Human parvovirus and aplastic crisis in chronic hemolytic anemias: a study of 24 observations. American journal of hematology. 1986;23(3):271-5.
101.   Saarinen UM, Chorba TL, Tattersall P, Young NS, Anderson LJ, Palmer E, et al. Human parvovirus B19-induced epidemic acute red cell aplasia in patients with hereditary hemolytic anemia. Blood. 1986;67(5):1411-7.
102.   Hanada T, Koike K, Takeya T, Nagasawa T, Matsunaga Y, Takita H. Human parvovirus B19-induced transient pancytopenia in a child with hereditary spherocytosis. British journal of haematology. 1988;70(1):113-5.
103.   Mabin DC, Chowdhury V. Aplastic crisis caused by human parvovirus in two patients with hereditary stomatocytosis. British journal of haematology. 1990;76(1):153-4.
104.   Duncan JR, Potter CB, Cappellini MD, Kurtz JB, Anderson MJ, Weatherall DJ. Aplastic crisis due to parvovirus infection in pyruvate kinase deficiency. Lancet. 1983;2(8340):14-6.
105.   Rechavi G, Vonsover A, Manor Y, Mileguir F, Shpilberg O, Kende G, et al. Aplastic crisis due to human B19 parvovirus infection in red cell pyrimidine-5'-nucleotidase deficiency. Acta haematologica. 1989;82(1):46-9.
106.   Serjeant GR, Topley JM, Mason K, Serjeant BE, Pattison JR, Jones SE, et al. Outbreak of aplastic crises in sickle cell anaemia associated with parvovirus-like agent. Lancet. 1981;2(8247):595-7.

107. Lakhani AK, Malkovska V, Bevan DH, Anderson MJ. Transient pancytopenia associated with parvovirus infection in paroxysmal nocturnal haemoglobinuria. Postgraduate medical journal. 1987;63(740):483-4.

108. Brown KE, Green SW, Antunez de Mayolo J, Bellanti JA, Smith SD, Smith TJ, et al. Congenital anaemia after transplacental B19 parvovirus infection. Lancet. 1994;343(8902):895-6.

109. Heegaard ED, Hasle H, Clausen N, Hornsleth A, Kerndrup GB. Parvovirus B19 infection and Diamond-Blackfan anaemia. Acta paediatrica. 1996;85(3):299-302.

110. Rugolotto S, Padovani EM, Sanna A, Chiaffoni GP, Marradi PL, Borgna-Pignatti C. Intrauterine anemia due to parvovirus B19: successful treatment with intravenous immunoglobulins. Haematologica. 1999;84(7):668-9.

111. Murray JC, Kelley PK, Hogrefe WR, McClain KL. Childhood idiopathic thrombocytopenic purpura: association with human parvovirus B19 infection. The American journal of pediatric hematology/oncology. 1994;16(4):314-9.

112. Potter CG, Potter AC, Hatton CS, Chapel HM, Anderson MJ, Pattison JR, et al. Variation of erythroid and myeloid precursors in the marrow and peripheral blood of volunteer subjects infected with human parvovirus (B19). The Journal of clinical investigation. 1987;79(5):1486-92.

113. Yoto Y, Kudoh T, Suzuki N, Katoh S, Matsunaga Y, Chiba S. Thrombocytopenia induced by human parvovirus B19 infections. European journal of haematology. 1993;50(5):255-7.

114. Heegaard ED, Rosthoj S, Petersen BL, Nielsen S, Karup Pedersen F, Hornsleth A. Role of parvovirus B19 infection in childhood idiopathic thrombocytopenic purpura. Acta paediatrica. 1999;88(6):614-7.

115. McClain K, Estrov Z, Chen H, Mahoney DH, Jr. Chronic neutropenia of childhood: frequent association with parvovirus infection and correlations with bone marrow culture studies. British journal of haematology. 1993;85(1):57-62.

116. Hanada T, Koike K, Hirano C, Takeya T, Suzuki T, Matsunaga Y, et al. Childhood transient erythroblastopenia complicated by thrombocytopenia and neutropenia. European journal of haematology. 1989;42(1):77-80.

117. Kynaston JA, West NC, Reid MM. A regional experience of red cell aplasia. European journal of pediatrics. 1993;152(4):306-8.

118. Nagai K, Morohoshi T, Kudoh T, Yoto Y, Suzuki N, Matsunaga Y. Transient erythroblastopenia of childhood with megakaryocytopenia associated with human parvovirus B19 infection. British journal of haematology. 1992;80(1):131-2.

119. Anderson MJ, Jones SE, Minson AC. Diagnosis of human parvovirus infection by dot-blot hybridization using cloned viral DNA. J Med Virol. 1985;15(2):163-72.

120. Mori J, Field AM, Clewley JP, Cohen BJ. Dot blot hybridization assay of B19 virus DNA in clinical specimens. Journal of clinical microbiology. 1989;27(3):459-64.

121. Jordan J, Tiangco B, Kiss J, Koch W. Human parvovirus B19: prevalence of viral DNA in volunteer blood donors and clinical outcomes of transfusion recipients. Vox sanguinis. 1998;75(2):97-102.

122. Lefrere JJ, Mariotti M, Thauvin M. B19 parvovirus DNA in solvent/detergent-treated anti-haemophilia concentrates. Lancet. 1994;343(8891):211-2.

123. McOmish F, Yap PL, Jordan A, Hart H, Cohen BJ, Simmonds P. Detection of parvovirus B19 in donated blood: a model system for screening by polymerase chain reaction. Journal of clinical microbiology. 1993;31(2):323-8.

124.   Cassinotti P, Siegl G. Quantitative evidence for persistence of human parvovirus B19 DNA in an immunocompetent individual. European journal of clinical microbiology & infectious diseases : official publication of the European Society of Clinical Microbiology. 2000;19(11):886-7.

125.   Musiani M, Zerbini M, Gentilomi G, Plazzi M, Gallinella G, Venturoli S. Parvovirus B19 clearance from peripheral blood after acute infection. The Journal of infectious diseases. 1995;172(5):1360-3.

126.   Patou G, Pillay D, Myint S, Pattison J. Characterization of a nested polymerase chain reaction assay for detection of parvovirus B19. Journal of clinical microbiology. 1993;31(3):540-6.

127.   Saal JG, Steidle M, Einsele H, Muller CA, Fritz P, Zacher J. Persistence of B19 parvovirus in synovial membranes of patients with rheumatoid arthritis. Rheumatology international. 1992;12(4):147-51.

128.   Cassinotti P, Burtonboy G, Fopp M, Siegl G. Evidence for persistence of human parvovirus B19 DNA in bone marrow. J Med Virol. 1997;53(3):229-32.

129.   Harris JW. Parvovirus B19 for the hematologist. American journal of hematology. 1992;39(2):119-30.

130.   Frickhofen N, Abkowitz JL, Safford M, Berry JM, Antunez-de-Mayolo J, Astrow A, et al. Persistent B19 parvovirus infection in patients infected with human immunodeficiency virus type 1 (HIV-1): a treatable cause of anemia in AIDS. Annals of internal medicine. 1990;113(12):926-33.

131.   Frickhofen N, Chen ZJ, Young NS, Cohen BJ, Heimpel H, Abkowitz JL. Parvovirus B19 as a cause of acquired chronic pure red cell aplasia. British journal of haematology. 1994;87(4):818-24.

132.   Koduri PR, Kumapley R, Valladares J, Teter C. Chronic pure red cell aplasia caused by parvovirus B19 in AIDS: use of intravenous immunoglobulin--a report of eight patients. American journal of hematology. 1999;61(1):16-20.

133.   Kurtzman G, Frickhofen N, Kimball J, Jenkins DW, Nienhuis AW, Young NS. Pure red-cell aplasia of 10 years' duration due to persistent parvovirus B19 infection and its cure with immunoglobulin therapy. N Engl J Med. 1989;321(8):519-23.

134.   Yu FH, Yarov-Yarovoy V, Gutman GA, Catterall WA. Overview of molecular relationships in the voltage-gated ion channel superfamily. Pharmacol Rev. 2005;57(4):387-95.

135.   Gutman GA, Chandy KG, Grissmer S, Lazdunski M, McKinnon D, Pardo LA, et al. International Union of Pharmacology. LIII. Nomenclature and molecular relationships of voltage-gated potassium channels. Pharmacol Rev. 2005;57(4):473-508.

136.   Hille B. Ion Channels of Excitable Cells. 3rd Edn ed. Sunderland, MA: Sinauer Associates; 2001.

137.   Felipe A, Vicente R, Villalonga N, Roura-Ferrer M, Martinez-Marmol R, Sole L, et al. Potassium channels: new targets in cancer therapy. Cancer Detect Prev. 2006;30(4):375-85.

138.   Sokolova O. Structure of cation channels, revealed by single particle electron microscopy. FEBS Lett. 2004;564(3):251-6.

139.   Carrington JC, Freed DD. Cap-independent enhancement of translation by a plant potyvirus 5' nontranslated region. Journal of virology. 1990;64(4):1590-7.

140.   Grizel AV, Glukhov GS, Sokolova OS. Mechanisms of activation of voltage-gated potassium channels. Acta naturae. 2014;6(4):10-26.

141.   Brandt F, Etchells SA, Ortiz JO, Elcock AH, Hartl FU, Baumeister W. The native 3D organization of bacterial polysomes. Cell. 2009;136(2):261-71.

142.   Myasnikov AG, Afonina ZA, Klaholz BP. Single particle and molecular assembly analysis of polyribosomes by single- and double-tilt cryo electron tomography. Ultramicroscopy. 2013;126:33-9.

143. Doyle DA, Morais Cabral J, Pfuetzner RA, Kuo A, Gulbis JM, Cohen SL, et al. The structure of the potassium channel: molecular basis of K+ conduction and selectivity. Science. 1998;280(5360):69-77.
144. Lu Z, Klem AM, Ramu Y. Coupling between voltage sensors and activation gate in voltage-gated K+ channels. The Journal of general physiology. 2002;120(5):663-76.
145. Lu Z, Klem AM, Ramu Y. Ion conduction pore is conserved among potassium channels. Nature. 2001;413(6858):809-13.
146. Labro AJ, Raes AL, Grottesi A, Van Hoorick D, Sansom MS, Snyders DJ. Kv channel gating requires a compatible S4-S5 linker and bottom part of S6, constrained by non-interacting residues. The Journal of general physiology. 2008;132(6):667-80.
147. Batulan Z, Haddad GA, Blunck R. An intersubunit interaction between S4-S5 linker and S6 is responsible for the slow off-gating component in Shaker K+ channels. J Biol Chem. 2010;285(18):14005-19.
148. Haddad GA, Blunck R. Mode shift of the voltage sensors in Shaker K+ channels is caused by energetic coupling to the pore domain. The Journal of general physiology. 2011;137(5):455-72.
149. Pischalnikova AV, Sokolova OS. The domain and conformational organization in potassium voltage-gated ion channels. Journal of neuroimmune pharmacology : the official journal of the Society on NeuroImmune Pharmacology. 2009;4(1):71-82.
150. Long SB, Campbell EB, Mackinnon R. Crystal structure of a mammalian voltage-dependent Shaker family K+ channel. Science. 2005;309(5736):897-903.
151. Swanson R, Marshall J, Smith JS, Williams JB, Boyle MB, Folander K, et al. Cloning and expression of cDNA and genomic clones encoding three delayed rectifier potassium channels in rat brain. Neuron. 1990;4(6):929-39.
152. Bielanska J, Hernandez-Losa J, Perez-Verdaguer M, Moline T, Somoza R, Ramon YCS, et al. Voltage-dependent potassium channels Kv1.3 and Kv1.5 in human cancer. Curr Cancer Drug Targets. 2009;9(8):904-14.
153. Stuhmer W, Ruppersberg JP, Schroter KH, Sakmann B, Stocker M, Giese KP, et al. Molecular basis of functional diversity of voltage-gated potassium channels in mammalian brain. EMBO J. 1989;8(11):3235-44.
154. Veh RW, Lichtinghagen R, Sewing S, Wunder F, Grumbach IM, Pongs O. Immunohistochemical localization of five members of the Kv1 channel subunits: contrasting subcellular locations and neuron-specific co-localizations in rat brain. Eur J Neurosci. 1995;7(11):2189-205.
155. Xu J, Wang P, Li Y, Li G, Kaczmarek LK, Wu Y, et al. The voltage-gated potassium channel Kv1.3 regulates peripheral insulin sensitivity. Proc Natl Acad Sci U S A. 2004;101(9):3112-7.
156. Villalonga N, Martinez-Marmol R, Roura-Ferrer M, David M, Valenzuela C, Soler C, et al. Cell cycle-dependent expression of Kv1.5 is involved in myoblast proliferation. Biochim Biophys Acta. 2008;1783(5):728-36.
157. Bielanska J, Hernandez-Losa J, Moline T, Somoza R, Cajal SR, Condom E, et al. Increased voltage-dependent K(+) channel Kv1.3 and Kv1.5 expression correlates with leiomyosarcoma aggressiveness. Oncol Lett.4(2):227-30.
158. Bielanska J, Hernandez-Losa J, Moline T, Somoza R, Ramon y Cajal S, Condom E, et al. Differential expression of Kv1.3 and Kv1.5 voltage-dependent K+ channels in human skeletal muscle sarcomas. Cancer Invest.30(3):203-8.
159. Grunnet M, Rasmussen HB, Hay-Schmidt A, Klaerke DA. The voltage-gated potassium channel subunit, Kv1.3, is expressed in epithelia. Biochim Biophys Acta. 2003;1616(1):85-94.

160.   Millar ID, Wang S, Brown PD, Barrand MA, Hladky SB. Kv1 and Kir2 potassium channels are expressed in rat brain endothelial cells. Pflugers Arch. 2008;456(2):379-91.
161.   Comes N, Bielanska J, Vallejo-Gracia A, Serrano-Albarras A, Marruecos L, Gomez D, et al. The voltage-dependent K(+) channels Kv1.3 and Kv1.5 in human cancer. Front Physiol.4:283.
162.   Tamkun MM, Knoth KM, Walbridge JA, Kroemer H, Roden DM, Glover DM. Molecular cloning and characterization of two voltage-gated K+ channel cDNAs from human ventricle. FASEB J. 1991;5(3):331-7.
163.   Chen WL, Huang XQ, Zhao LY, Li J, Chen JW, Xiao Y, et al. Involvement of Kv1.5 protein in oxidative vascular endothelial cell injury. PloS one. 2012;7(11):e49758.
164.   Coma M, Vicente R, Busquets S, Carbo N, Tamkun MM, Lopez-Soriano FJ, et al. Impaired voltage-gated K+ channel expression in brain during experimental cancer cachexia. FEBS Lett. 2003;536(1-3):45-50.
165.   Vicente R, Escalada A, Coma M, Fuster G, Sanchez-Tillo E, Lopez-Iglesias C, et al. Differential voltage-dependent K+ channel responses during proliferation and activation in macrophages. J Biol Chem. 2003;278(47):46307-20.
166.   Lesage F, Attali B, Lazdunski M, Barhanin J. Developmental expression of voltage-sensitive K+ channels in mouse skeletal muscle and C2C12 cells. FEBS Lett. 1992;310(2):162-6.
167.   Yuan XJ, Wang J, Juhaszova M, Golovina VA, Rubin LJ. Molecular basis and function of voltage-gated K+ channels in pulmonary arterial smooth muscle cells. Am J Physiol. 1998;274(4 Pt 1):L621-35.
168.   DeCoursey TE, Chandy KG, Gupta S, Cahalan MD. Voltage-gated K+ channels in human T lymphocytes: a role in mitogenesis? Nature. 1984;307(5950):465-8.
169.   Deutsch C, Lee SC. Cell volume regulation in lymphocytes. Ren Physiol Biochem. 1988;11(3-5):260-76.
170.   Storey NM, Gomez-Angelats M, Bortner CD, Armstrong DL, Cidlowski JA. Stimulation of Kv1.3 potassium channels by death receptors during apoptosis in Jurkat T lymphocytes. J Biol Chem. 2003;278(35):33319-26.
171.   Bonnet S, Archer SL, Allalunis-Turner J, Haromy A, Beaulieu C, Thompson R, et al. A mitochondria-K+ channel axis is suppressed in cancer and its normalization promotes apoptosis and inhibits cancer growth. Cancer cell. 2007;11(1):37-51.
172.   Zhou Q, Kwan HY, Chan HC, Jiang JL, Tam SC, Yao X. Blockage of voltage-gated K+ channels inhibits adhesion and proliferation of hepatocarcinoma cells. International journal of molecular medicine. 2003;11(2):261-6.
173.   Kupper J, Bowlby MR, Marom S, Levitan IB. Intracellular and extracellular amino acids that influence C-type inactivation and its modulation in a voltage-dependent potassium channel. Pflugers Arch. 1995;430(1):1-11.
174.   Preussat K, Beetz C, Schrey M, Kraft R, Wolfl S, Kalff R, et al. Expression of voltage-gated potassium channels Kv1.3 and Kv1.5 in human gliomas. Neuroscience letters. 2003;346(1-2):33-6.
175.   Xu J, Koni PA, Wang P, Li G, Kaczmarek L, Wu Y, et al. The voltage-gated potassium channel Kv1.3 regulates energy homeostasis and body weight. Hum Mol Genet. 2003;12(5):551-9.
176.   Grissmer S, Nguyen AN, Aiyar J, Hanson DC, Mather RJ, Gutman GA, et al. Pharmacological characterization of five cloned voltage-gated K+ channels, types Kv1.1, 1.2, 1.3, 1.5, and 3.1, stably expressed in mammalian cell lines. Mol Pharmacol. 1994;45(6):1227-34.
177.   Vennekamp J, Wulff H, Beeton C, Calabresi PA, Grissmer S, Hansel W, et al. Kv1.3-blocking 5-phenylalkoxypsoralens: a new class of immunomodulators. Mol Pharmacol. 2004;65(6):1364-74.

178.   Leonard RJ, Garcia ML, Slaughter RS, Reuben JP. Selective blockers of voltage-gated K+ channels depolarize human T lymphocytes: mechanism of the antiproliferative effect of charybdotoxin. Proc Natl Acad Sci U S A. 1992;89(21):10094-8.

179.   Garcia-Calvo M, Leonard RJ, Novick J, Stevens SP, Schmalhofer W, Kaczorowski GJ, et al. Purification, characterization, and biosynthesis of margatoxin, a component of Centruroides margaritatus venom that selectively inhibits voltage-dependent potassium channels. J Biol Chem. 1993;268(25):18866-74.

180.   Cahalan MD, Chandy KG. Ion channels in the immune system as targets for immunosuppression. Curr Opin Biotechnol. 1997;8(6):749-56.

181.   Decher N, Pirard B, Bundis F, Peukert S, Baringhaus KH, Busch AE, et al. Molecular basis for Kv1.5 channel block: conservation of drug binding sites among voltage-gated K+ channels. J Biol Chem. 2004;279(1):394-400.

182.   Du YM, Zhang XX, Tu DN, Zhao N, Liu YJ, Xiao H, et al. Molecular determinants of Kv1.5 channel block by diphenyl phosphine oxide-1. J Mol Cell Cardiol.48(6):1111-20.

183.   Wulff H, Calabresi PA, Allie R, Yun S, Pennington M, Beeton C, et al. The voltage-gated Kv1.3 K(+) channel in effector memory T cells as new target for MS. The Journal of clinical investigation. 2003;111(11):1703-13.

184.   Tschritter O, Machicao F, Stefan N, Schafer S, Weigert C, Staiger H, et al. A new variant in the human Kv1.3 gene is associated with low insulin sensitivity and impaired glucose tolerance. The Journal of clinical endocrinology and metabolism. 2006;91(2):654-8.

185.   Olson TM, Alekseev AE, Liu XK, Park S, Zingman LV, Bienengraeber M, et al. Kv1.5 channelopathy due to KCNA5 loss-of-function mutation causes human atrial fibrillation. Hum Mol Genet. 2006;15(14):2185-91.

186.   Kubo Y, Baldwin TJ, Jan YN, Jan LY. Primary structure and functional expression of a mouse inward rectifier potassium channel. Nature. 1993;362(6416):127-33.

187.   Tinker A, Jan YN, Jan LY. Regions responsible for the assembly of inwardly rectifying potassium channels. Cell. 1996;87(5):857-68.

188.   Preisig-Muller R, Schlichthorl G, Goerge T, Heinen S, Bruggemann A, Rajan S, et al. Heteromerization of Kir2.x potassium channels contributes to the phenotype of Andersen's syndrome. Proc Natl Acad Sci U S A. 2002;99(11):7774-9.

189.   Hibino H, Inanobe A, Furutani K, Murakami S, Findlay I, Kurachi Y. Inwardly rectifying potassium channels: their structure, function, and physiological roles. Physiological reviews. 2010;90(1):291-366.

190.   Matsuda H, Saigusa A, Irisawa H. Ohmic conductance through the inwardly rectifying K channel and blocking by internal Mg2+. Nature. 1987;325(7000):156-9.

191.   Vandenberg CA. Inward rectification of a potassium channel in cardiac ventricular cells depends on internal magnesium ions. Proc Natl Acad Sci U S A. 1987;84(8):2560-4.

192.   Lopatin AN, Makhina EN, Nichols CG. Potassium channel block by cytoplasmic polyamines as the mechanism of intrinsic rectification. Nature. 1994;372(6504):366-9.

193.   Yamada M, Kurachi Y. Spermine gates inward-rectifying muscarinic but not ATP-sensitive K+ channels in rabbit atrial myocytes. Intracellular substance-mediated mechanism of inward rectification. J Biol Chem. 1995;270(16):9289-94.

194.   Kubo Y, Murata Y. Control of rectification and permeation by two distinct sites after the second transmembrane region in Kir2.1 K+ channel. The Journal of physiology. 2001;531(Pt 3):645-60.

195.   Taglialatela M, Ficker E, Wible BA, Brown AM. C-terminus determinants for Mg2+ and polyamine block of the inward rectifier K+ channel IRK1. EMBO J. 1995;14(22):5532-41.
196.   Taglialatela M, Wible BA, Caporaso R, Brown AM. Specification of pore properties by the carboxyl terminus of inwardly rectifying K+ channels. Science. 1994;264(5160):844-7.
197.   Yang J, Jan YN, Jan LY. Control of rectification and permeation by residues in two distinct domains in an inward rectifier K+ channel. Neuron. 1995;14(5):1047-54.
198.   Lu T, Nguyen B, Zhang X, Yang J. Architecture of a K+ channel inner pore revealed by stoichiometric covalent modification. Neuron. 1999;22(3):571-80.
199.   Minor DL, Jr., Masseling SJ, Jan YN, Jan LY. Transmembrane structure of an inwardly rectifying potassium channel. Cell. 1999;96(6):879-91.
200.   Pegan S, Arrabit C, Zhou W, Kwiatkowski W, Collins A, Slesinger PA, et al. Cytoplasmic domain structures of Kir2.1 and Kir3.1 show sites for modulating gating and rectification. Nature neuroscience. 2005;8(3):279-87.
201.   Henry P, Pearson WL, Nichols CG. Protein kinase C inhibition of cloned inward rectifier (HRK1/KIR2.3) K+ channels expressed in Xenopus oocytes. The Journal of physiology. 1996;495 (Pt 3):681-8.
202.   Dart C, Leyland ML. Targeting of an A kinase-anchoring protein, AKAP79, to an inwardly rectifying potassium channel, Kir2.1. J Biol Chem. 2001;276(23):20499-505.
203.   Ito H, Tsuchimochi H, Tada Y, Kurachi Y. Phosphorylation-independent inhibition by intracellular cyclic nucleotides of brain inwardly rectifying K+ current expressed in Xenopus oocytes. FEBS Lett. 1997;402(1):12-6.
204.   Du X, Zhang H, Lopes C, Mirshahi T, Rohacs T, Logothetis DE. Characteristic interactions with phosphatidylinositol 4,5-bisphosphate determine regulation of kir channels by diverse modulators. J Biol Chem. 2004;279(36):37271-81.
205.   Boyer SB, Slesinger PA, Jones SV. Regulation of Kir2.1 channels by the Rho-GTPase, Rac1. Journal of cellular physiology. 2009;218(2):385-93.
206.   Leyland ML, Dart C. An alternatively spliced isoform of PSD-93/chapsyn 110 binds to the inwardly rectifying potassium channel, Kir2.1. J Biol Chem. 2004;279(42):43427-36.
207.   Liu Y, Liu D, Heath L, Meyers DM, Krafte DS, Wagoner PK, et al. Direct activation of an inwardly rectifying potassium channel by arachidonic acid. Mol Pharmacol. 2001;59(5):1061-8.
208.   Donaldson MR, Jensen JL, Tristani-Firouzi M, Tawil R, Bendahhou S, Suarez WA, et al. PIP2 binding residues of Kir2.1 are common targets of mutations causing Andersen syndrome. Neurology. 2003;60(11):1811-6.
209.   Rohacs T, Chen J, Prestwich GD, Logothetis DE. Distinct specificities of inwardly rectifying K(+) channels for phosphoinositides. J Biol Chem. 1999;274(51):36065-72.
210.   Romanenko VG, Fang Y, Byfield F, Travis AJ, Vandenberg CA, Rothblat GH, et al. Cholesterol sensitivity and lipid raft targeting of Kir2.1 channels. Biophysical journal. 2004;87(6):3850-61.
211.   Wischmeyer E, Doring F, Karschin A. Acute suppression of inwardly rectifying Kir2.1 channels by direct tyrosine kinase phosphorylation. J Biol Chem. 1998;273(51):34063-8.
212.   Vicente R, Coma M, Busquets S, Moore-Carrasco R, Lopez-Soriano FJ, Argiles JM, et al. The systemic inflammatory response is involved in the regulation of K(+) channel expression in brain via TNF-alpha-dependent and -independent pathways. FEBS Lett. 2004;572(1-3):189-94.
213.   Sampson LJ, Leyland ML, Dart C. Direct interaction between the actin-binding protein filamin-A and the inwardly rectifying potassium channel, Kir2.1. J Biol Chem. 2003;278(43):41988-97.

214.	Beeler GW, Jr., Reuter H. Voltage clamp experiments on ventricular myocarial fibres. The Journal of physiology. 1970;207(1):165-90.

215.	Kurachi Y. Voltage-dependent activation of the inward-rectifier potassium channel in the ventricular cell membrane of guinea-pig heart. The Journal of physiology. 1985;366:365-85.

216.	McAllister RE, Noble D. The time and voltage dependence of the slow outward current in cardiac Purkinje fibres. The Journal of physiology. 1966;186(3):632-62.

217.	Rougier O, Vassort G, Stampfli R. Voltage clamp experiments on frog atrial heart muscle fibres with the sucrose gap technique. Pflugers Archiv fur die gesamte Physiologie des Menschen und der Tiere. 1968;301(2):91-108.

218.	Noma A, Nakayama T, Kurachi Y, Irisawa H. Resting K conductances in pacemaker and non-pacemaker heart cells of the rabbit. The Japanese journal of physiology. 1984;34(2):245-54.

219.	Zobel C, Cho HC, Nguyen TT, Pekhletski R, Diaz RJ, Wilson GJ, et al. Molecular dissection of the inward rectifier potassium current (IK1) in rabbit cardiomyocytes: evidence for heteromeric co-assembly of Kir2.1 and Kir2.2. The Journal of physiology. 2003;550(Pt 2):365-72.

220.	Adams DJ, Hill MA. Potassium channels and membrane potential in the modulation of intracellular calcium in vascular endothelial cells. Journal of cardiovascular electrophysiology. 2004;15(5):598-610.

221.	Nilius B, Droogmans G. Ion channels and their functional role in vascular endothelium. Physiological reviews. 2001;81(4):1415-59.

222.	Nilius B, Schwarz G, Droogmans G. Modulation by histamine of an inwardly rectifying potassium channel in human endothelial cells. The Journal of physiology. 1993;472:359-71.

223.	von Beckerath N, Dittrich M, Klieber HG, Daut J. Inwardly rectifying K+ channels in freshly dissociated coronary endothelial cells from guinea-pig heart. The Journal of physiology. 1996;491 (Pt 2):357-65.

224.	Kwan HY, Leung PC, Huang Y, Yao X. Depletion of intracellular Ca2+ stores sensitizes the flow-induced Ca2+ influx in rat endothelial cells. Circulation research. 2003;92(3):286-92.

225.	Wellman GC, Bevan JA. Barium inhibits the endothelium-dependent component of flow but not acetylcholine-induced relaxation in isolated rabbit cerebral arteries. The Journal of pharmacology and experimental therapeutics. 1995;274(1):47-53.

226.	Bradley KK, Jaggar JH, Bonev AD, Heppner TJ, Flynn ER, Nelson MT, et al. Kir2.1 encodes the inward rectifier potassium channel in rat arterial smooth muscle cells. The Journal of physiology. 1999;515 (Pt 3):639-51.

227.	Zaritsky JJ, Eckman DM, Wellman GC, Nelson MT, Schwarz TL. Targeted disruption of Kir2.1 and Kir2.2 genes reveals the essential role of the inwardly rectifying K(+) current in K(+)-mediated vasodilation. Circulation research. 2000;87(2):160-6.

228.	Brown DA, Gahwiler BH, Griffith WH, Halliwell JV. Membrane currents in hippocampal neurons. Progress in brain research. 1990;83:141-60.

229.	Takahashi T. Inward rectification in neonatal rat spinal motoneurones. The Journal of physiology. 1990;423:47-62.

230.	Day M, Carr DB, Ulrich S, Ilijic E, Tkatch T, Surmeier DJ. Dendritic excitability of mouse frontal cortex pyramidal neurons is shaped by the interaction among HCN, Kir2, and Kleak channels. The Journal of neuroscience : the official journal of the Society for Neuroscience. 2005;25(38):8776-87.

231.	Horio Y, Morishige K, Takahashi N, Kurachi Y. Differential distribution of classical inwardly rectifying potassium channel mRNAs in the brain: comparison of IRK2 with IRK1 and IRK3. FEBS Lett. 1996;379(3):239-43.

232.   Wilson GF, Chiu SY. Ion channels in axon and Schwann cell membranes at paranodes of mammalian myelinated fibers studied with patch clamp. The Journal of neuroscience : the official journal of the Society for Neuroscience. 1990;10(10):3263-74.

233.   Mi H, Deerinck TJ, Jones M, Ellisman MH, Schwarz TL. Inwardly rectifying K+ channels that may participate in K+ buffering are localized in microvilli of Schwann cells. The Journal of neuroscience : the official journal of the Society for Neuroscience. 1996;16(8):2421-9.

234.   Raab-Graham KF, Radeke CM, Vandenberg CA. Molecular cloning and expression of a human heart inward rectifier potassium channel. Neuroreport. 1994;5(18):2501-5.

235.   Plaster NM, Tawil R, Tristani-Firouzi M, Canun S, Bendahhou S, Tsunoda A, et al. Mutations in Kir2.1 cause the developmental and episodic electrical phenotypes of Andersen's syndrome. Cell. 2001;105(4):511-9.

236.   Konig S, Hinard V, Arnaudeau S, Holzer N, Potter G, Bader CR, et al. Membrane hyperpolarization triggers myogenin and myocyte enhancer factor-2 expression during human myoblast differentiation. J Biol Chem. 2004;279(27):28187-96.

237.   Fischer-Lougheed J, Liu JH, Espinos E, Mordasini D, Bader CR, Belin D, et al. Human myoblast fusion requires expression of functional inward rectifier Kir2.1 channels. The Journal of cell biology. 2001;153(4):677-86.

238.   Leichtle A, Rauch U, Albinus M, Benohr P, Kalbacher H, Mack AF, et al. Electrophysiological and molecular characterization of the inward rectifier in juxtaglomerular cells from rat kidney. The Journal of physiology. 2004;560(Pt 2):365-76.

239.   Lang F, Rehwald W. Potassium channels in renal epithelial transport regulation. Physiological reviews. 1992;72(1):1-32.

240.   Tawil R, Ptacek LJ, Pavlakis SG, DeVivo DC, Penn AS, Ozdemir C, et al. Andersen's syndrome: potassium-sensitive periodic paralysis, ventricular ectopy, and dysmorphic features. Annals of neurology. 1994;35(3):326-30.

241.   Bendahhou S, Donaldson MR, Plaster NM, Tristani-Firouzi M, Fu YH, Ptacek LJ. Defective potassium channel Kir2.1 trafficking underlies Andersen-Tawil syndrome. J Biol Chem. 2003;278(51):51779-85.

242.   Lange PS, Er F, Gassanov N, Hoppe UC. Andersen mutations of KCNJ2 suppress the native inward rectifier current IK1 in a dominant-negative fashion. Cardiovascular research. 2003;59(2):321-7.

243.   Lopes CM, Zhang H, Rohacs T, Jin T, Yang J, Logothetis DE. Alterations in conserved Kir channel-PIP2 interactions underlie channelopathies. Neuron. 2002;34(6):933-44.

244.   Schimpf R, Wolpert C, Gaita F, Giustetto C, Borggrefe M. Short QT syndrome. Cardiovascular research. 2005;67(3):357-66.

245.   Brown KE, Young NS, Liu JM. Molecular, cellular and clinical aspects of parvovirus B19 infection. Crit Rev Oncol Hematol. 1994;16(1):1-31.

246.   Brown KE, Hibbs JR, Gallinella G, Anderson SM, Lehman ED, McCarthy P, et al. Resistance to parvovirus B19 infection due to lack of virus receptor (erythrocyte P antigen). N Engl J Med. 1994;330(17):1192-6.

247.   Kuhl U, Pauschinger M, Bock T, Klingel K, Schwimmbeck CP, Seeberg B, et al. Parvovirus B19 infection mimicking acute myocardial infarction. Circulation. 2003;108(8):945-50.

248.   Bock CT, Klingel K, Kandolf R. Human parvovirus B19-associated myocarditis. N Engl J Med. 2010;362(13):1248-9.

249.   Lupescu A, Bock CT, Lang PA, Aberle S, Kaiser H, Kandolf R, et al. Phospholipase A2 activity-dependent stimulation of Ca2+ entry by human parvovirus B19 capsid protein VP1. J Virol. 2006;80(22):11370-80.
250.   Almilaji A, Szteyn K, Fein E, Pakladok T, Munoz C, Elvira B, et al. Down-regulation of Na/K+ atpase activity by human parvovirus B19 capsid protein VP1. Cellular physiology and biochemistry : international journal of experimental cellular physiology, biochemistry, and pharmacology. 2013;31(4-5):638-48.
251.   Rabini RA, Fumelli P, Zolese G, Amler E, Salvolini E, Staffolani R, et al. Modifications induced by plasma from insulin-dependent diabetic patients and by lysophosphatidylcholine on human Na+,K(+)-adenosine triphosphatase. J Clin Endocrinol Metab. 1998;83(7):2405-10.
252.   Wickenden A. K(+) channels as therapeutic drug targets. Pharmacol Ther. 2002;94(1-2):157-82.
253.   Felipe A, Bielanska J, Comes N, Vallejo A, Roig S, Ramon YC, et al. Targeting the voltage-dependent K(+) channels Kv1.3 and Kv1.5 as tumor biomarkers for cancer detection and prevention. Curr Med Chem. 2012;19(5):661-74.
254.   Munoz C, Tovolli RH, Sopjani M, Alesutan I, Lam RS, Seebohm G, et al. Activation of voltage gated K(+) channel Kv1.5 by beta-catenin. Biochemical and biophysical research communications. 2012;417(2):692-6.
255.   Tyan L, Sopjani M, Dermaku-Sopjani M, Schmid E, Yang W, Xuan NT, et al. Inhibition of voltage-gated K+ channels in dendritic cells by rapamycin. American journal of physiology Cell physiology. 2010;299(6):C1379-85.
256.   Munoz C, Pakladok T, Almilaji A, Elvira B, Decher N, Shumilina E, et al. Up-regulation of Kir2.1 (KCNJ2) by the serum & glucocorticoid inducible SGK3. Cellular physiology and biochemistry : international journal of experimental cellular physiology, biochemistry, and pharmacology. 2014;33(2):491-500.
257.   Henrion U, Zumhagen S, Steinke K, Strutz-Seebohm N, Stallmeyer B, Lang F, et al. Overlapping cardiac phenotype associated with a familial mutation in the voltage sensor of the KCNQ1 channel. Cellular physiology and biochemistry : international journal of experimental cellular physiology, biochemistry, and pharmacology. 2012;29(5-6):809-18.
258.   Hosseinzadeh Z, Bhavsar SK, Lang F. Downregulation of ClC-2 by JAK2. Cell Physiol Biochem. 2012;29(5-6):737-42.
259.   Munoz C, Sopjani M, Dermaku-Sopjani M, Almilaji A, Foller M, Lang F. Downregulation of the osmolyte transporters SMIT and BGT1 by AMP-activated protein kinase. Biochemical and biophysical research communications. 2012;422(3):358-62.
260.   Almilaji A, Munoz C, Hosseinzadeh Z, Lang F. Upregulation of Na+,Cl(-)-coupled betaine/gamma-amino-butyric acid transporter BGT1 by Tau tubulin kinase 2. Cell Physiol Biochem. 2013;32(2):334-43.
261.   Almilaji A, Pakladok T, Guo A, Munoz C, Foller M, Lang F. Regulation of the glutamate transporter EAAT3 by mammalian target of rapamycin mTOR. Biochemical and biophysical research communications. 2012;421(2):159-63.
262.   Hosseinzadeh Z, Bhavsar SK, Lang F. Down-Regulation of the Myoinositol Transporter SMIT by JAK2. Cell Physiol Biochem. 2012;30(6):1473-80.
263.   Mia S, Munoz C, Pakladok T, Siraskar G, Voelkl J, Alesutan I, et al. Downregulation of Kv1.5 K Channels by the AMP-Activated Protein Kinase. Cell Physiol Biochem. 2012;30(4):1039-50.
264.   Pathare G, Foller M, Daryadel A, Mutig K, Bogatikov E, Fajol A, et al. OSR1-Sensitive Renal Tubular Phosphate Reabsorption. Kidney Blood Press Res. 2012;36(1):149-61.

265.   Bogatikov E, Munoz C, Pakladok T, Alesutan I, Shojaiefard M, Seebohm G, et al. Up-Regulation of Amino Acid Transporter SLC6A19 Activity and Surface Protein Abundance by PKB/Akt and PIKfyve. Cellular physiology and biochemistry : international journal of experimental cellular physiology, biochemistry, and pharmacology. 2012;30(6):1538-46.
266.   Hosseinzadeh Z, Luo D, Sopjani M, Bhavsar SK, Lang F. Down-regulation of the epithelial Na(+) channel ENaC by Janus kinase 2. The Journal of membrane biology. 2014;247(4):331-8.
267.   Munoz C, Almilaji A, Setiawan I, Foller M, Lang F. Up-regulation of the inwardly rectifying K(+) channel Kir2.1 (KCNJ2) by protein kinase B (PKB/Akt) and PIKfyve. The Journal of membrane biology. 2013;246(3):189-97.
268.   Hosseinzadeh Z, Bhavsar SK, Lang F. Downregulation of ClC-2 by JAK2. Cell Physiol Biochem. 2012;29(5-6):737-42.
269.   Shojaiefard M, Hosseinzadeh Z, Bhavsar SK, Lang F. Downregulation of the creatine transporter SLC6A8 by JAK2. The Journal of membrane biology. 2012;245(3):157-63.
270.   Warsi J, Elvira B, Hosseinzadeh Z, Shumilina E, Lang F. Downregulation of chloride channel ClC-2 by Janus kinase 3. The Journal of membrane biology. 2014;247(5):387-93.
271.   Almilaji A, Munoz C, Hosseinzadeh Z, Lang F. Upregulation of Na+,Cl(-)-coupled betaine/gamma-amino-butyric acid transporter BGT1 by Tau tubulin kinase 2. Cell Physiol Biochem. 2013;32(2):334-43.
272.   Pakladok T, Hosseinzadeh Z, Lebedeva A, Alesutan I, Lang F. Upregulation of the Na(+)-coupled phosphate cotransporters NaPi-IIa and NaPi-IIb by B-RAF. The Journal of membrane biology. 2014;247(2):137-45.
273.   Mia S, Munoz C, Pakladok T, Siraskar G, Voelkl J, Alesutan I, et al. Downregulation of Kv1.5 K Channels by the AMP-Activated Protein Kinase. Cell Physiol Biochem. 2012;30(4):1039-50.
274.   Pathare G, Foller M, Daryadel A, Mutig K, Bogatikov E, Fajol A, et al. OSR1-Sensitive Renal Tubular Phosphate Reabsorption. Kidney Blood Press Res. 2012;36(1):149-61.
275.   Bock CT, Klingel K, Aberle S, Duechting A, Lupescu A, Lang F, et al. Human parvovirus B19: a new emerging pathogen of inflammatory cardiomyopathy. Journal of veterinary medicine B, Infectious diseases and veterinary public health. 2005;52(7-8):340-3.
276.   Magro CM, Nuovo G, Ferri C, Crowson AN, Giuggioli D, Sebastiani M. Parvoviral infection of endothelial cells and stromal fibroblasts: a possible pathogenetic role in scleroderma. Journal of cutaneous pathology. 2004;31(1):43-50.
277.   Hogg RC, Bandelier F, Benoit A, Dosch R, Bertrand D. An automated system for intracellular and intranuclear injection. Journal of neuroscience methods. 2008;169(1):65-75.
278.   Gurdon JB, Lane CD, Woodland HR, Marbaix G. Use of frog eggs and oocytes for the study of messenger RNA and its translation in living cells. Nature. 1971;233(5316):177-82.
279.   Almilaji A, Honisch S, Liu G, Elvira B, Ajay SS, Hosseinzadeh Z, et al. Regulation of the voltage gated K channel Kv1.3 by recombinant human klotho protein. Kidney Blood Press Res. 2014;39(6):609-22.
280.   Almilaji A, Munoz C, Elvira B, Fajol A, Pakladok T, Honisch S, et al. AMP-activated protein kinase regulates hERG potassium channel. Pflugers Arch. 2013;465(11):1573-82.
281.   Ahmed M, Salker MS, Elvira B, Umbach AT, Fakhri H, Saeed AM, et al. SPAK Sensitive Regulation of the Epithelial Na Channel ENaC. Kidney Blood Press Res. 2015;40(4):335-43.
282.   Bhavsar SK, Hosseinzadeh Z, Brenner D, Honisch S, Jilani K, Liu G, et al. Energy-sensitive regulation of Na+/K+-ATPase by Janus kinase 2. Am J Physiol Cell Physiol. 2014;306(4):C374-84.
283.   Canaan S, Zadori Z, Ghomashchi F, Bollinger J, Sadilek M, Moreau ME, et al. Interfacial enzymology of parvovirus phospholipases A2. J Biol Chem. 2004;279(15):14502-8.

284.   Dorsch S, Liebisch G, Kaufmann B, von Landenberg P, Hoffmann JH, Drobnik W, et al. The VP1 unique region of parvovirus B19 and its constituent phospholipase A2-like activity. J Virol. 2002;76(4):2014-8.

285.   Lang F, Busch GL, Ritter M, Volkl H, Waldegger S, Gulbins E, et al. Functional significance of cell volume regulatory mechanisms. Physiol Rev. 1998;78(1):247-306.

286.   Lang F. Mechanisms and significance of cell volume regulation. J Am Coll Nutr. 2007;26(5 Suppl):613S-23S.

287.   Summers J, Jones SE, Anderson MJ. Characterization of the genome of the agent of erythrocyte aplasia permits its classification as a human parvovirus. The Journal of general virology. 1983;64 (Pt 11):2527-32.

288.   Ahmed M, Almilaji A, Munoz C, Elvira B, Shumilina E, Bock CT, et al. Down-regulation of K(+) channels by human parvovirus B19 capsid protein VP1. Biochem Biophys Res Commun. 2014;450(4):1396-401.

Declaration

I hereby declare that this thesis is my original work and it has been written by me. this work contains no material which has been accepted for the award of any other degree in my name in any university and to the best of my knowledge and belief, contains no material previously published or written by another person, except where due reference has been made in the text.

The experimental work was carried out in Institute of Physiology I, University of Tübingen

The result presented in figure 6, 7 and 8 were generated by Ahmad Almilaji and all the other results in this thesis were generated by me.

Part of this thesis has been published:

Down-regulation of inwardly rectifying Kir2.1 K+ channels by human parvovirus B19 capsid protein VP1.
Ahmed M, Elvira B, Almilaji A, Bock CT, Kandolf R, Lang F.
J Membr Biol. 2015 Apr;248(2):223-9. doi: 10.1007/s00232-014-9762-9. Epub 2014 Dec 9.
Down-regulation of K^+ channels by human parvovirus B19 capsid protein VP1.
Ahmed M, Almilaji A, Munoz C, Elvira B, Shumilina E, Bock CT, Kandolf R, Lang F.
Biochem Biophys Res Commun. 2014 Aug 8;450(4):1396-401. doi: 10.1016/j.bbrc.2014.07.003. Epub 2014 Jul 7.

Musaab Sedig Ahmed

Curriculum Vitae

Personal information

Name: Musaab Sedig Ahmed

Address: Institute of Physiology, University of Tübingen, Gmelin str.5, Tübingen 72076, Germany

 Mobile: 015217507384

 E-mail: musaabsab@yahoo.com

Nationality: Sudanese

Date of birth: 3.1.1979

Gender : Male

Work experience

September 2013 up to now: MD student, institute of Physiology, University of Tübingen, Tübingen, Germany

February 2011 up to August 2013: Lecturer, Department of Physiology, Faculty of Medicine, Red Sea University, Sudan

July 2010- January 2011: Teaching assistant in the Department of Physiology, Faculty of Medicine, Red Sea University, Sudan

June 2008- June 2010: Tutor in the Department of Physiology, Faculty of Medicine, International University of Africa, Sudan

February 2007- February 2008: General practitioner in the medical commission of the military service, Sudan.

September 2005- January 2007: House officer in the Sudanese hospitals

Education and training

2008 – 2010: MSc in Physiology, University of Khartoum, Khartoum, Sudan

2004 :Bachelor of Medicine and Surgery (MBBS),Upper Nile University, Sudan

1996: Secondary school certificate, Ministry of education, State of Qatar

Workshops

28th of November – 2nd December 2010: Course design and management, Educational Development Centre, Faculty of Medicine, University of Khartoum

26th – 30th December 2010: Assessment and evaluation, Educational Development Centre, Faculty of Medicine, University of Khartoum

13th – 17th March 2011: Teaching and learning, Educational Development Centre, Faculty of Medicine, University of Khartoum

Conferences

22nd- 23rd February 2010: The 2nd clinical neurology course , Soba University Hospital, University of Khartoum, Sudan provided by The Sudanese Society for Neurological Sciences

24th – 25th February 2010:The 3rd Sudanese neurosciences Conference, Faculty of Medicine, University of Khartoum provided by The Sudanese Society for Neurological Sciences

Invited posters

94th Annual meeting of the German Physiological Society (Down-regulation of inwardly rectifying Kir2.1 K+ channels by human parvovirus B19 capsid protein VP1) Magdeburg, Germany 2015.

My Publications

SPAK Sensitive Regulation of the Epithelial Na Channel ENaC.
Ahmed M, Salker MS, Elvira B, Umbach AT, Fakhri H, Saeed AM, Shumilina E, Hosseinzadeh Z, Lang F.
Kidney Blood Press Res. 2015 Jun 14;40(4):335-343. [Epub ahead of print]

Regulation of the voltage gated K channel Kv1.3 by recombinant human klotho protein.
Almilaji A, Honisch S, Liu G, Elvira B, Ajay SS, Hosseinzadeh Z, Ahmed M, Munoz C, Sopjani M, Lang F.
Kidney Blood Press Res. 2014;39(6):609-22. doi: 10.1159/000368472. Epub 2014 Dec 15.

Down-regulation of inwardly rectifying Kir2.1 K+ channels by human parvovirus B19 capsid protein VP1.
Ahmed M, Elvira B, Almilaji A, Bock CT, Kandolf R, Lang F.
J Membr Biol. 2015 Apr;248(2):223-9. doi: 10.1007/s00232-014-9762-9. Epub 2014 Dec 9.

Down-regulation of K$^+$ channels by human parvovirus B19 capsid protein VP1.
Ahmed M, Almilaji A, Munoz C, Elvira B, Shumilina E, Bock CT, Kandolf R, Lang F.
Biochem Biophys Res Commun. 2014 Aug 8;450(4):1396-401. doi: 10.1016/j.bbrc.2014.07.003. Epub 2014 Jul 7.

Acknowledgment

Iam very grateful for my supervisor Prof.Dr. Florian Lang for his encouragement, support and continuous help. iam highly thankful for his valuable advices and his wise recommendations.

Iam very thankful for Dr. Zohreh hosseinzadeh, Uwe Schuler, Dr. Peter Dreischer and Dr. Lisann Pelzl for their support, caring and positive attitude.

I would also to thank all my colleagues in Institute of Physiology I, University of Tübingen for the wonderful time we spend in working together. I was really happy and proud to be part of this excellent group and to meet and work with these intelligent people.